ACS NANO

www.acsnano.org

REVIEW

Quantum and Classical Exceptional Points at the Nanoscale: Properties and Applications

Yu-Wei Lu, Wei Li, and Xue-Hua Wang*

Cite This: https://doi.org/10.1021/acsnano.4c15648

Read Online

ACCESS | Metrics & More | Article Recommendations

ABSTRACT: Exceptional points (EPs) are the spectral singularities and one of the central concepts of non-Hermitian physics, originating from the inevitable energy exchange with the surrounding environment. EPs exist in diverse physical systems and give rise to many counterintuitive effects, offering rich opportunities to control the dynamics and alter the properties of optical, electronic, acoustic, and mechanical states. The last two decades have witnessed the flourishing of non-Hermitian physics and associated applications related to coalesced eigenstates at EPs in a plethora of classical systems. While stemming from the quantum mechanism, the implementation of EPs in real quantum systems still faces challenges of tuning and stabilizing the systems at EPs, as well as the additional noises that hinder the observation of relevant phenomena. This review mainly focuses on summarizing the current efforts and opportunities offered by quantum EPs that result from or produce observable quantum effects. We introduce the concepts of Hamiltonian and Liouvillian EPs in the quantum regime and focus on their different properties in connection with quantum jumps and decoherence. We then provide a comprehensive discussion covering the theoretical and experimental advances in accessing EPs in diverse quantum systems and platforms. Special attention is paid to EP-based quantum-optics applications with state-of-art technologies. Finally, we present a discussion on the existing challenges of constructing quantum EPs at the nanoscale and an outlook on the fundamental science and applied technologies of quantum EPs, aiming to provide valuable insights for future research and building quantum devices with high performance and advanced functionalities.

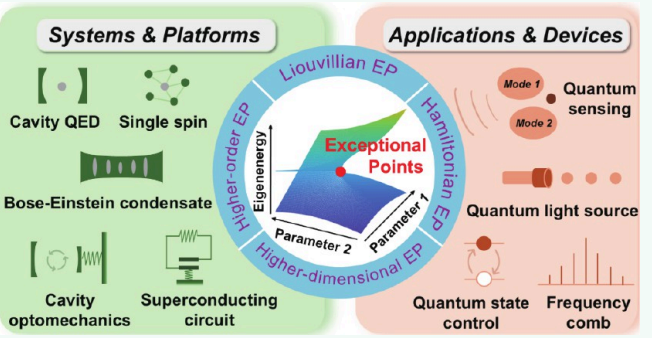

KEYWORDS: *exceptional points, non-Hermitian physics, eigenstates, open quantum systems, quantum states, quantum sensing, nonclassical light, spontaneous emission, quantum devices*

1. INTRODUCTION

The concept of non-Hermiticity and related counterintuitive aspects have raised intense attention in the past two decades and have been extensively explored in the interdisciplinary field of non-Hermitian physics combined with different kinds of nonconservative systems not limited to the optical[1−4] and acoustic[5] arrangements where wave dynamics dominates, but even electronic,[6,7] mechanical[8,9] systems and the diffusive system of heat exist.[10] What makes this class of physical systems so attractive is the notion of singularities known as exceptional points (EPs) and the associated phase transition of parity-time (PT) symmetry. These unique features of non-Hermitian systems have no Hermitian counterpart and lead to a plethora of intriguing behaviors due to the dramatically altered overall response near the EPs and exotic functionalities based on the great ability of state control offered by the EPs. The EPs thus provide a new strategy to develop novel devices by exploiting loss, which is traditionally considered impossible to attain high performance.

While flourishing in non-Hermitian classical systems, the idea of the EPs originated from quantum mechanics, which was initially developed based on Hermitian operator algebra with the assumption of energy conservation. It guarantees the properties of real eigenenergies spectrum and orthogonal eigenstates of a Hamiltonian but demands the closure of the quantum system. Though the whole system can be conservative, the interaction between the specific subsystems of interest and the surrounding environment, accompanied by

Received: November 3, 2024
Revised: April 21, 2025
Accepted: April 22, 2025

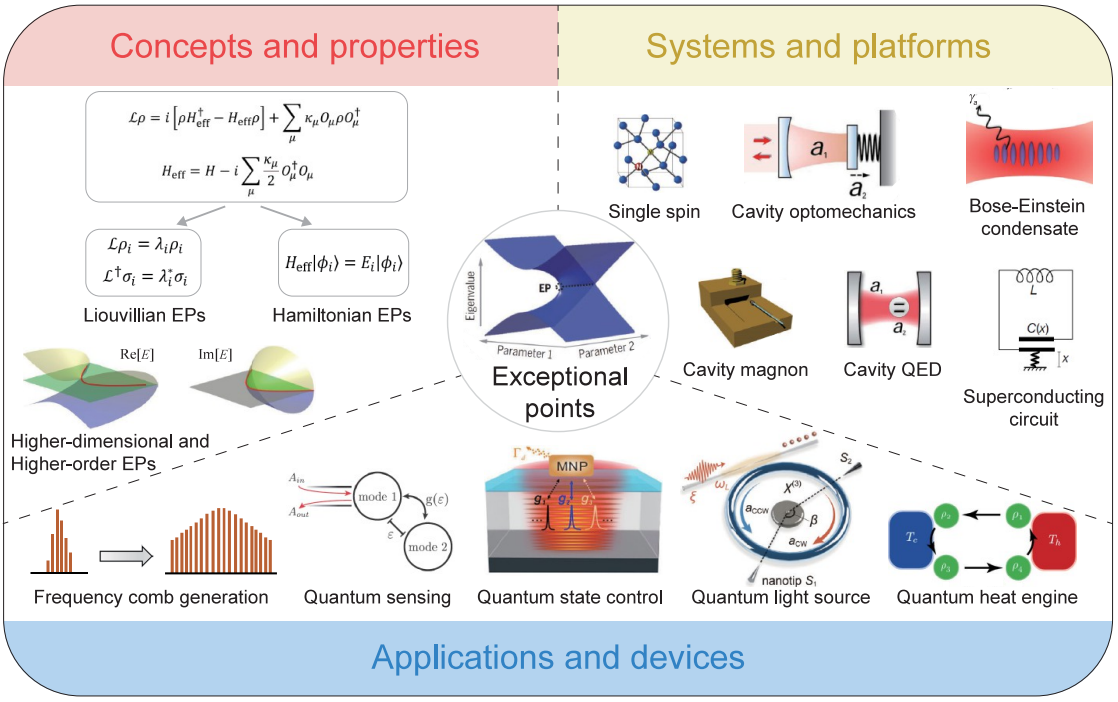

Figure 1. Key concepts and implementations of exceptional points (EPs) in various quantum systems and the quantum-optics applications based on quantum EPs. Schematic illustration of EPs is reproduced from ref 3. Copyright 2021 AAAS. The definitions of symbols in equations are given in Section 2. Schematic illustrations of the higher-dimensional and higher-order EPs are reproduced from ref 64. Copyright 2024 Springer Nature. The exemplary platforms for constructing quantum EPs: (1) Single spin. Reproduced from ref 54. Copyright 2019 AAAS. (2) Cavity optomechanics. Reproduced from ref 3. Copyright 2021 AAAS. (3) Bose−Einstein condensate. Reproduced from ref 81. Copyright 2022 The Authors. Published by Springer Nature in partnership with the University of New South Wales, licensed under CC-BY 4.0. (4) Cavity magnon. Reproduced from ref 60. Copyright 2017 The Authors. Published by Springer Nature and licensed under CC-BY 4.0. (5) Cavity QED. Reproduced from ref 3. Copyright 2021 AAAS. (6) Superconducting circuit. Reproduced from ref 82. Copyright 2022 Springer Nature. The representative quantum-optics applications and devices for quantum EPs (see Section 3 for detailed discussion): (1) Frequency comb. Reproduced from ref 47. Copyright 2024 Springer Nature. (2) Quantum sensing. Reproduced from ref 69. Copyright 2022 American Chemical Society. (3) Quantum state control. Reproduced from ref 42. Copyright 2023 American Physical Society. (4) Quantum light source. Reproduced from ref 33. Copyright 2022 Wiley-VCH GmbH. (5) Quantum heat engine. Reproduced from ref 83. Copyright 2017 American Physical Society.

either a growth or a loss of energy, will violate the fundamental premise of Hermiticity. Such open quantum systems are ubiquitously found in realistic physical settings and require proper treatment of emerging non-Hermiticity. The early attempt is to introduce the non-Hermitian Hamiltonian that accounts for the dissipation resulting from nonconservative interactions.[11−13] In the non-Hermitian description, an open quantum system exhibits complex-valued eigenenergies, with the imaginary part representing the broadening of resonances and the decay rate of eigenstates. The non-Hermitian component is not a small perturbation of the original Hermitian Hamiltonian, whereas it exhibits fundamentally distinct features. It is found that when a non-Hermitian Hamiltonian satisfies PT symmetry, the eigenenergies spectrum can be purely real, while the underlying state space is skewed.[14−17] Notably, at the transition points between the PT-symmetry phase and the PT-symmetry broken phase, not only can the eigenenergies be degenerate but also the associated eigenstates become completely parallel. Degeneracies with a higher order may exhibit richer topological features of complicated energy structures.[18−20] These branch-point singularities of parameter space are called EPs,[1,3,21,22] which are essentially different from the conventional degeneracies of Hermitian counterparts. These findings and the established theoretical foundation extend quantum mechanics into a new regime and open an avenue to non-Hermitian physics.

Though revolutionary in physical concept, the EPs of non-Hermitian Hamiltonian emerging at the mean-field level neglect the quantum jumps term that leads to the instantaneous switching between quantum states, and thus has a serious impact on the quantum dynamics.[23] The dynamics of the open quantum systems can be correctly described by the Lindblad formalism, where the Liouvillian superoperator takes the effect of quantum jumps into account. As discovered recently, the Liouvillian superoperator may not share the same eigenenergies spectrum as the corresponding non-Hermitian Hamiltonian without quantum jumps.[24] Therefore, the EPs of Liouvillian superoperator in general do not accord with that of the non-Hermitian Hamiltonian, but the dimensionality of the underlying parameter space can be reduced at the EPs in both situations, which is also anticipated to yield exotic behaviors. In this review, the classical EPs are referred to as the exceptional degeneracies of non-Hermitian Hamiltonian, while the exceptional degeneracies that have quantum origin or produce the observable quantum effects are called quantum EPs. Quantum EPs can dramatically render the dynamics of the open quantum systems and the properties of quantum states, including the quantum state transfer,[8,25,26] entanglement,[27−29] interference,[30,31] decoherence,[32] the inten-

https://doi.org/10.1021/acsnano.4c15648
ACS Nano XXXX, XXX, XXX−XXX

sity distribution and photon statistics of light.[33,34] Moreover, the quantum EPs can significantly modify the fundamental physical and biochemical processes, such as spontaneous emission,[35−39] strong light-matter interactions,[40−42] and quantum chemistry,[43−46] demonstrating great potential in developing functional nanodevices with advantageous performance, for instance, quantum light sources,[33,40] frequency combs,[47] quantum battery,[48,49] quantum heat engine,[50] and quantum sensor,[51,52] to name a few. So far, the quantum EPs have been implemented in diverse quantum systems, ranging from single natural and artificial spins,[53−57] nanophotonic platforms,[35,40,42,58] cavity optomechanics,[9,59] to cavity magnons[47,60,61] and superconducting circuits[62,63] (see Figure 1 for exemplary quantum systems). These fruitful results have greatly deepened the understanding of the quantum effect of the EPs in non-Hermitian systems and facilitated technological breakthroughs for practical applications.

Despite the quantum EPs being of both science interest and applied importance, the isolated EP poses a great challenge on the experimental observation of the EPs' features and related striking effect in quantum systems. The precise control of system parameters is required to access the EPs, which is demanding for quantum systems with a nanometer size and working at cryogenic temperatures. Especially, the fabrication errors and structure imperfections are inevitable at the nanoscale. These difficulties can be resolved to some extent by constructing higher-dimensional EPs, including but not limited to the exceptional line,[56,64,65] exceptional surface,[35,61,66,67] and exceptional chamber,[68] which manifest greater tolerance against the variation of system parameters. However, the general methods and technologies of monitoring the quantum dynamics at the EPs and achieving dynamical control are highly desirable but are still scarce. Furthermore, the effect of quantum and thermal noises has a significant influence on the quantum dynamics at the few-quanta level and should be considered in the development of EP-based quantum devices, which may set the fundamental limit of performance. For instance, recent theoretical studies have proved that an EP-based quantum sensor offers no advantage in enhancing the signal-to-noise ratio due to the existence of quantum and thermal noises.[69−74] In addition, though the physical concept of optical gain in the semiclassical approach is widely adopted in non-Hermitian classical photonics, it remains ambiguous in the quantum regime.[75−77] Therefore, the exploration of the quantum EPs is not simply migrating the setups of non-Hermitian classical systems and the conclusions drawn from non-Hermitian Hamiltonians but encourages more efforts devoted to unveiling the unique features of the quantum EPs and discovering unexpected behaviors belonging to open quantum systems.

Over the past few years, tremendous progress has been achieved in the theory and the experimental implementations of the quantum EPs, and it provides a new perspective of loss, which was thought to be detrimental but can also benefit the applications in quantum information processing, quantum communication, and computation.[25,28,33,47,78−80] This review reflects upon the fruitful results, ongoing endeavors, and future trends of quantum EPs. We first introduce the basic concepts of the EPs in the Liouvillian superoperator and non-Hermitian Hamiltonian and their properties with respect to the degeneracy and dimensionality. Guided by the theoretical background, we briefly revisit the achievement of demonstrating the analogous quantum effects of the EPs in non-Hermitian classical photonics, where the PT symmetry can be flexibly established by employing an optical gain. Subsequently, we discuss the implementations and applications of quantum EPs in diverse quantum systems and platforms from the perspectives of exotic quantum manipulation and advanced quantum devices with novel functionalities. We focus on the ability and potential of the EPs to render the quantum nature of quantum states. Based on the theoretical and experimental advancements, we summarize the current challenges and rich opportunities in harnessing the characteristics of quantum EPs for advanced quantum technologies. Finally, we prospect promising directions of quantum EPs for future research.

2. THEORY OF EXCEPTIONAL POINTS IN NON-HERMITIAN QUANTUM SYSTEMS

The non-Hermiticity is initially introduced in the study of alpha decay, where the imaginary part of complex eigenenergies describes the decay of a quantum state to the outside of a nucleus, and thus is related to the line width of the corresponding nuclear resonances.[11,12] In a subsequent work, the complex potential function is adopted in the single-particle Schrödinger equation to model the scattering between neutrons and nuclei, where the imaginary part accounts for the neutron absorption in potential.[13] In these early works of open quantum systems, the introduction of the non-Hermiticity is phenomenological, and the quantum dissipation is captured by the effective non-Hermitian Hamiltonian at the mean-field level, where the effects of the quantum jumps are neglected. A rigorous approach, such as Lindblad master equation or Heisenberg−Langevin equation,[84] is needed to describe the dynamics of the open quantum systems.

2.1. Lindblad Master Equation and Liouvillian EPs.

The time evolution of an open quantum system interacting with a Markovian environment follows the Lindblad master equation

$$\mathcal{L}\rho(t) = \frac{\partial}{\partial t}\rho(t) = i[\rho(t), H] + \sum_{\mu} \mathcal{D}[O_\mu] \tag{1}$$

where $\mathcal{L}$ is the Liouvillian superoperator and $\rho(t)$ is the density matrix of system at time t. $\mathcal{D}[O_\mu]$ is the Lindblad dissipator for operator O_μ and takes the form as $\mathcal{D}[O_\mu] = \kappa_\mu[O_\mu\rho(t)O_\mu^\dagger - O_\mu^\dagger O_\mu\rho(t)/2 - \rho(t)O_\mu^\dagger O_\mu/2]$, where the dissipation to the environment is at a rate κ_μ. $\mathcal{D}[O_\mu]$ can be divided into two parts according to different physical meanings: $\mathcal{D}[O_\mu] = \mathcal{D}_j[O_\mu] + \mathcal{D}_n[O_\mu]$, with $\mathcal{D}_j[O_\mu] = \kappa_\mu O_\mu\rho(t)O_\mu^\dagger$ describing the effects of quantum jump that lead to the abrupt stochastic switching between quantum states and $\mathcal{D}_n[O_\mu] = -\kappa_\mu[O_\mu^\dagger O_\mu\rho(t) + \rho(t)O_\mu^\dagger O_\mu]/2$ being the contribution of nonunitary dissipation.

The spectrum of the Liouvillian superoperator $\mathcal{L}$ contains the information about an open quantum system.[23,85,86] Because $\mathcal{L}$ can be non-Hermitian, it admits both the left and right eigenmatrices. The right eigenmatrices are defined by $\mathcal{L}\rho_i = \lambda_i\rho_i$,[24] where ρ_i is the normalized eigenmatrices related to eigenenergy λ_i and satisfies $\mathrm{Tr}[\rho_i^\dagger\rho_i] = 1$. Similarly, the left eigenmatrices and associated eigenenergies are defined by $\mathcal{L}^\dagger\sigma_i = \lambda_i^*\sigma_i$. The orthogonality is lost for different left or right eigenmatrices, i.e., $\mathrm{Tr}[\rho_i^\dagger\rho_i] \neq \delta_{ij}$ and $\mathrm{Tr}[\sigma_j\sigma_i^\dagger] \neq \delta_{ji}$, but the

https://doi.org/10.1021/acsnano.4c15648
ACS Nano XXXX, XXX, XXX−XXX

left and right eigenmatrices of $\mathcal{L}$ are biorthogonal, i.e., $\mathrm{Tr}[\sigma_i \rho_i] = \delta_{ij}$.[87]

In the Lindblad formalism (eq 1), a Liouvillian EP (LEP) is the degenerate point of parameter space where at least two eigenmatrices and associated eigenenergies coalesce. The presence of the LEP modifies the quantum dynamics toward the steady state, and thus the LEPs can be revealed by studying the dynamics of an open quantum system. For example, two kinds of LEPs originated from the competition of nonunitary energy dissipation and decoherence and the pure decoherence have been revealed by evaluating the oscillation frequency and decay rate of the transient dynamics of a transmon superconducting circuit.[62] The first kind of LEP results from the different loss of the y and z Pauli operators of qubit achieved by tailoring the spectral density of cavity, while the latter arises from the unbalanced losses of two coherences of the density matrix through the inclusion of a reference level; see the schematic and results shown in Figure 3h–k for further elaboration. As applications, the LEPs can be utilized to optimize the quantum dynamics since the quantum system at the LEPs approaches its steady state faster than the non-LEP case.[88,89] This feature can be harnessed to achieve the precise dynamical control of quantum thermal machines and has been experimentally demonstrated in a recent work,[90] which shows that the LEPs are responsible for the Mpemba effect in quantum thermodynamics, a counterintuitive phenomenon that a far-from-equilibrium quantum state can relax toward equilibrium faster than a state closer to equilibrium. In addition, the optimized quantum state steering based on LEPs has been proposed for the two-level quantum systems with weak measurements[91] and in the Floquet regime.[92]

Before concluding this subsection, two points of LEPs should be noted. One is that the existing works of the EPs are confined to the Markovian limit, i.e., the case of memoryless environment, which is valid, for example, when the coupling between the system and environment is sufficiently weak, while for the structured environment or in the non-Markovian regime, recent work has shown that the condition of these non-Markovian EPs is in general different from that of the Markovian limit and adjustable by tailoring the spectral density of the environment. The findings filled the gap between the non-Hermitian physics and nonperturbative quantum electrodynamics.[93]

On the other hand, it is worth mentioning that the Heisenberg–Langevin equation is an alternative approach for investigating the dissipative dynamics through the noise operators produced by fluctuations. The equivalence of quantum dynamics described by the Heisenberg–Langevin equation and Lindblad master equation guarantees the consistency of the EPs found by these two different approaches.[94] However, for a quantum system with N-dimensional Hilbert space, the corresponding Liouville space is of dimension N^2. Therefore, the eigensystem (i.e., eigenvalues and eigenvectors) analysis of the Lindblad master equation is challenging for multilevel or multimode systems with high-dimensional Hilbert space. In this case, the Heisenberg–Langevin equation may be advantageous, with a higher efficiency compared to the Lindblad master equation since it finds the eigensystem from the dynamic matrix of the equation of measurable operators. The approach of Heisenberg-Langevin equation has been applied to analyze the eigensystem of two nonlinearly interacting damped and amplified bosonic modes coupled to reservoirs[95] and the multimode bosonic system with quadratic Hamiltonian, which shows the ability of simulating arbitrary nonunitary processes in a quantum nonlinear optical circuit through symplectic transformation.[96]

2.2. Effective Hamiltonian in Semiclassical Limit and Its EPs. By separating the quantum jumps term from the Lindblad dissipator, the master equation can be rewritten in the following form:

$$\frac{\partial}{\partial t}\rho(t) = i[\rho(t), H] - i\sum_{\mu}\{\rho(t), H_d\} + \sum_{\mu}\mathcal{D}_j[O_\mu] \tag{2}$$

where $H_d = -i\frac{\kappa_\mu}{2}O_\mu^\dagger O_\mu$ is an anti-Hermitian operator satisfying $H_d^\dagger = -H_d$. Therefore, the above equation becomes $\partial\rho(t)/\partial t = i[\rho(t)H_{\mathrm{eff}}^\dagger - H_{\mathrm{eff}}\rho(t)] + \sum_\mu \mathcal{D}_j[O_\mu]$, where the contribution of nonunitary energy dissipation H_d is incorporated into an effective non-Hermitian Hamiltonian H_{eff}, which takes the form as

$$H_{\mathrm{eff}} = H - i\sum_{\mu}\frac{\kappa_\mu}{2}O_\mu^\dagger O_\mu \tag{3}$$

which indicates that H_{eff} together with the quantum jumps term can retrieve the quantum dynamics given by Lindblad formalism. If we assume that all the quantum states of the system exhibit a semiclassical nature, then the effect of quantum jumps can be negligible, which yields $L'\rho(t) \equiv \partial\rho(t)/\partial t = i[\rho(t)H_{\mathrm{eff}}^\dagger - H_{\mathrm{eff}}\rho(t)]$. In this semiclassical limit, the non-Hermitian features of an open quantum system can be well described by H_{eff}. In the quantum regime, weak excitation is a typical situation in which the effective non-Hermitian Hamiltonian H_{eff} can be applied. Though imposing strict restrictions on the applications in open quantum systems, the approach of the effective non-Hermitian Hamiltonian lays the foundation for studying non-Hermitian physics in various kinds of classical wave systems, such as acoustics, mechanics, electronics, and photonics. Many intriguing effects of the non-Hermitian systems are rooted in the hidden PT symmetry of the corresponding non-Hermitian Hamiltonian, which is first revealed by a pioneering work in the studies of non-Hermitian physics made by Carl Bender and Stefan Boettcher.[14] The PT symmetry can induce spectral degeneracy at transition points of complex-to-real spectral phase transition, which in general exhibits a complex value due to the nonunitarity of the effective non-Hermitian Hamiltonian. The right eigenstates $|\phi_i\rangle$ and associated eigenenergies E_i of the effective non-Hermitian Hamiltonian H_{eff} can be found by solving $H_{\mathrm{eff}}|\phi_i\rangle = E_i|\phi_i\rangle$. The spectral degeneracies of H_{eff} where the eigenenergies and eigenstates simultaneously coincide correspond to the occurrence of an EP termed a Hamiltonian EP (HEP). The HEPs and LEPs are only equivalent in the semiclassical limit but show fundamentally distinct properties in the quantum regime. For instance, two kinds of EPs may exist in the same quantum system, while the parameters of the HEPs and LEPs are different, and the order of the LEPs is generally higher than the HEPs.[85] This feature results in a special case where an open quantum system can exhibit the LEPs but no HEPs if the EPs are induced by the quantum jumps.[24] We highlight that the quantum EPs discussed here not only refer to the LEPs in open quantum systems but also include those existing in the subsystems and demonstrating

https://doi.org/10.1021/acsnano.4c15648
ACS Nano XXXX, XXX, XXX–XXX

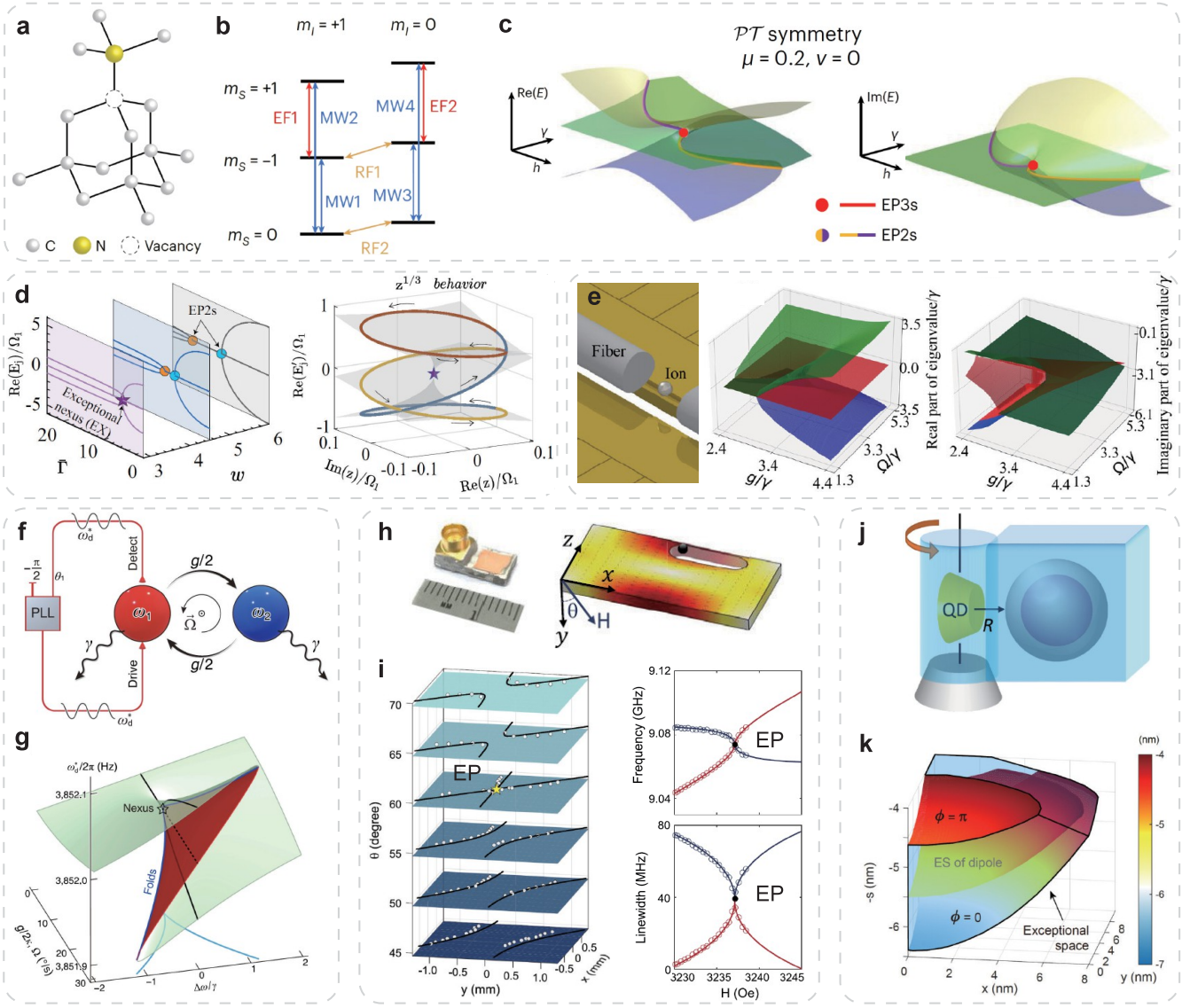

Figure 2. Higher-order and higher-dimensional EPs in quantum systems. Atomic structure (a) and energy levels (b) of the NV center. Panel (c) is the realization of third-order isolated EPs based on the NV center within the second-order exceptional line under PT symmetry.[64] Adapted with permission from ref 64. Copyright 2024 Springer Nature. (d) Exceptional nexus (EX) in the two-dimensional parameter space of Bose−Einstein condensates without symmetry. EX forms through the coalescence of two exceptional arcs consisting of EP2s (left). The corresponding real part of eigenenergies is shown as the function of z, demonstrating anisotropic perturbation effects near the EX (right).[56] Adapted with permission from ref 56. Copyright 2024 American Physical Society. (e) Illustration of experimental setting with the ion and fiber-based cavity (left). The real (middle) and imaginary (right) parts of the eigenvalues are plotted as a function of g and Ω. The green, red, and blue sheets correspond to three eigenenergies surfaces.[113] Adapted with permission from ref 113. Copyright 2023 American Institute of Physics. (f) Schematic of the phase-tracked coupled two-mode system, where the phase-locked-loop is employed to act as an external force driving one of the modes, while another mode remains free. (g) The eigenenergies as a function of degeneracy condition $\Delta\omega$ and coupling strength g. The green (red) region of the surface represents the stable (unstable) regime.[105] Adapted with permission from ref 105. Copyright 2023 The Authors. Published by Springer Nature, licensed under CC-BY 4.0. (h) Microwave and magnonic cavity and the simulated cavity magnetic fields for TE_{101} mode. (i) Slices of the exceptional surface in the 3D parameter space (left) and the cross sections of the Riemann surfaces at the exceptional saddle point (right).[61] Adapted with permission from ref 61. Copyright 2019 American Physical Society. (j) A plasmonic nanoparticle strongly coupled to a large asymmetric quantum dot (QD). (k) The rotation of QD produces a three-dimensional space of second-order EPs called exceptional chamber.[68] Adapted with permission from ref 68. Copyright 2021 The Authors. Published by De Gruyter, licensed under CC-BY 4.0.

quantum effects. For example, the EPs of an optical cavity are classical, but can have a significant impact on the quantum dynamics of the cavity quantum electrodynamics (QED) systems by altering the local density of states that defines the number of available optical modes for a quantum emitter to decay.[35,37,38,41,97,98] A detailed discussion of this example can be found in the next section.

2.3. Connecting Liouvillian and Hamiltonian EPs via Hybrid Liouvillian Formalism.

The complete suppression of the quantum jumps term $\mathcal{D}_j[O_\mu]$ in eq 2 leads to the transition from the LEP in the quantum regime to the HEP in a semiclassical limit. This can be achieved by postselecting the trajectories where no quantum jump took place through the perfect probe on the environment of the quantum system.[99]

https://doi.org/10.1021/acsnano.4c15648
ACS Nano XXXX, XXX, XXX−XXX

However, the perfect postselection is impossible due to the finite efficiency of a real detector, and the effect of quantum jumps can be captured by the hybrid Liouvillian formalism:

$$\mathcal{L}_H\rho(t) = i[\rho(t)H_{\text{eff}}^{\dagger} - H_{\text{eff}}\rho(t)] + q\sum_{\mu}\kappa_\mu O_\mu\rho(t)O_\mu^{\dagger} \quad (4)$$

where the tunable parameter $q = 1 - \eta$ depends on the detector efficiency η. Particularly, $\eta = 0$ corresponds to no postselection and LEPs, while $\eta = 1$ represents the perfect postselection and the HEPs in the semiclassical limit. Equation 4 shows that the hybrid Liouvillian formalism can describe the dissipative dynamics in the general case of imperfect postselection with $0 < \eta < 1$, establishing a connection of EPs between these two limits. The interplay of nonunitary energy dissipation and quantum jumps in the hybrid Liouvillian formalism has been experimentally validated in a transmon superconducting circuit,[55,62] where the elimination of trials with quantum jumps is achieved by the single-shot readout of the transmon state through the probe of the copper cavity. The enhanced decoherence and the breakdown of adiabaticity have been found at the LEPs through the quantum state tomography. Shilan Abo et al. presented a quite different experimental investigation of LEPs using quantum process tomography on IBM quantum processors,[100] where the Liouvillians can be completely reconstructed. The circuits were designed to simulate the decay of a single qubit through competing channels, resulting in LEPs but no HEPs. The study confirmed the theoretical predictions that the LEPs can exist independently of the HEPs due to the effect of quantum jumps.[24]

2.4. Degeneracy and Dimensionality of EPs. In the context of general properties, we consider the degeneracy (order) and dimensionality of the EPs. The k-fold degeneracy of the eigenenergies and eigenstates gives rise to a kth-order EP (EPk). In the vicinity of a kth-order EP, the response of the system to perturbation ε is dominant by the term with respect to $\varepsilon^{1/k}$; for small perturbation with $\varepsilon \ll 1$, the contribution of this term is considerably larger than the linear term about ε.[101−104] Therefore, the sensitivity of EP-based sensors is enhanced by the factor of $\varepsilon^{1/k-1}$, which tends to infinity as ε approaches to zero. The EP-based sensors are thus expected to beat the metrology limit of Hermitian counterparts, and the enhanced sensitivity is ultimately limited by the dissipation to resolve the frequency splitting in the spectrum. In addition, the nontrivial topological features are expected to be more abundant as the order of the EPs increases.[18] These advantages have triggered the pursuit of constructing higher-order quantum EPs.

However, the experimental observation of higher-order EPs requires the synchronous manipulation of multiple system parameters, imposing great challenges on the atomic and molecular systems. The feasible methods to realize the higher-order EPs are summarized as follows: 1) Coherently coupled systems with phase-locked-loop: As demonstrated in a mechanical disk resonator with a pair of standing-wave modes, the phase-tracked steady states of the system exhibit bistability with folds at the boundaries. A cusp singularity at the merged two folds shows the cubic root response even if the system consists of coupled two modes.[105] The introduced phase-tracking method establishes higher-order EPs without the requirement of nonlinear potential energies, offering the opportunities of building advanced singular devices with simple and controllable elements. 2) Unidirectional coupling: This kind of nonreciprocal interaction allows one to concatenate the subsystems without modifying their original eigenvalues, enabling the creation of an arbitrarily high order of the EPs on demand.[104,106] It is a straightforward method to construct desirable higher-order EPs. For example, a hierarchical approach through unidirectional coupling was proposed for the whispering-gallery-mode (WGM) cavity supporting an exceptional surface (see Figure 4i for the schematic): Each WGM cavity with EPs of order $k = 2$ is coupled in a unidirectional way through the waveguide resulting in a composite system with EPs of order $2k$.[107,108] Therefore, the unidirectional coupling is a scalable protocol for realizing the higher-order EPs with passive resonators in diverse platforms. 3) Coalescence of low-order EPs: Interestingly, higher-order EPs can also be created through the interaction between the multiple EPs. As the system parameters vary, multiple EPs can collide and emerge into higher-order exceptional singularities.[109] A paradigm is the coalescence of multiple exceptional arcs consisting of EP2s to produce an exceptional nexus,[5,56] which is an EP3 and has a different topological nature from original EP2s. The creation of higher-order EPs through the coalescence of low-order EPs can greatly reduce the system parameters that require meticulous tuning, providing a feasible scheme to realize the higher-order EPs in experiments. 4) Symmetry-protected higher-order EPs: it is shown that the third-order EPs in generical only require two tunable parameters in the presence of either a PT symmetry or a generalized chiral symmetry.[110,111] Furthermore, these different symmetries also yield distinct topologies of EPs.

The higher-order EPs were achieved on diverse platforms. Recently, the breakthrough has been achieved in an experimental work of a nitrogen-vacancy (NV) center in diamond, as shown in Figure 2a, where an EP3s line appears due to the introduction of the PT symmetry and pseudochirality.[64] The applied microwave and electric field pulses enable precise control of the electronic and nuclear spin states of the NV center (see Figure 2b), and thus the coalescence of eigenvalues and eigenstates at the EP3s can be observed in a single spin system at the atomic scale, as shown in Figure 2c. Very recently, the EP3s have also been observed in the ultracold atoms featuring a three-state system[56] (see Figure 2d), quantum thermal machine,[88] and the quantum optical systems simulating a two-dimensional non-Hermitian system in the reciprocal space with single photons.[112] These approaches can be applied to explore topological physics related to higher-order EPs and offer new potentials for applications in quantum technologies.

One of the most promising platforms for implementing higher-order quantum EPs is the nanophotonic structures. For instance, the 3-fold spectral degeneracies of the coupled cavity modes lead to the formation of the EP3s, which can be exploited to enhance the rates of resonance energy transfer and spontaneous emission by a factor of 8.[37,114] Therefore, the cavity architectures featuring higher-order EPs provides an ideal test bed for studying the exotic QED behaviors at the quantum EPs by interacting with the nanoscale quantum emitters, including ions[113] (see Figure 2e for an example), molecules,[40] and quantum dots.[37,98] Moreover, the interplay between the optical and mechanical modes constitutes a cavity optomechanics system, where the higher-order EPs can form by introducing the gain in one of the modes,[59,115,116] opening

https://doi.org/10.1021/acsnano.4c15648
ACS Nano XXXX, XXX, XXX−XXX

up new avenues of manipulating the phonons in optomechanical devices.

Besides the degeneracy, dimensionality (or geometry) is also another important characteristic of the EPs. Compared to the isolated EPs, the higher-dimensional EPs in the geometries of line, ring, and surface can offer more degrees of freedom in the parameter space, thus providing advantages over isolated EPs in the ease of access, great tunability, and robustness against the structure imperfections and experimental uncertainties. Generally, the presence of multiple symmetries is crucial in the creation of the higher-dimensional EPs in non-Hermitian systems,[110,111] which can extend an isolated EP to interesting geometries in the parameter space, yielding the exceptional lines,[64] surfaces,[61,66] etc. However, if a non-Hermitian system possesses redundant degrees of freedom, where the parameter space is n-dimensional with $n > 2(k - 1)$, then the higher-dimensional EPks will naturally arise. For instance, a recent study has reported that an exceptional surface can be formed by a collection of anisotropic EPs in a magnon polariton system with four-dimensional synthetic space,[61] as shown in Figure 2f and g. It is worth mentioning that in the standard configuration of the cavity QED system, the parameter regions of weak and strong light-matter interactions are mediated through an EP2. Taking the strongly coupled plasmon-quantum dot system as an example, the coupling strength between the plasmon and a nonspherical quantum dot depends on their frequencies detuning and the location and dipole orientation of quantum dot; thus the system exhibits a three-dimensional exceptional chamber consisting of EP2s in parameter space,[68] as illustrated in Figure 2h and i. Another special kind of higher-dimensional EP2s is the so-called chiral EPs, which is an exceptional surface embedded in the parameter space resulting from the chiral (i.e., unidirectional) coupling between the two components of the system.[66,117,118] One of the typical realizations of the chiral EPs in a photonic structure is the WGM microcavity coupled to a semi-infinite waveguide with a mirror at the end. The mirror reflection leads to unidirectional coupling between the pair of degenerate WGM modes with opposite propagating directions, which produces the chiral EPs. A microcavity featuring chiral EPs, which is called CEP cavity hereafter, is attractive in studying the cavity QED at quantum EPs due to the ability of tuning the spontaneous emission and suppressing the decoherence of a quantum emitter.[35,40,98,119] Moreover, the CEP cavity shows an advantage that the unavoidable fabrication errors merely shift the operating point along the exceptional surface, and thus the system manifests great robustness against a large class of undesired perturbations and can access the quantum EPs with ease.[66] These findings indicate the new potential of higher-dimensional EPs in practical applications.

2.5. Diabolical Degeneracies and Hybrid Diabolical-Exceptional Points. The occurrence of degenerate eigeneneregies (eigenvalues) is not rare in both Hermitian and non-Hermitian systems. The unique feature of EPs in non-Hermitian systems is the simultaneous coalescence of eigeneneregies and the corresponding eigenstates (eigenvectors). On the contrary, the degeneracy involving only the eigeneneregies, while the associated eigenstates remain orthogonal, is dubbed the diabolical points (DPs).[120] For a simple two-parameter real Hamiltonian, the DP is a double-cone connection between two surface of energy levels. The DPs can exist in both Hermitian and non-Hermitian systems since the degeneracy of eigeneneregies does not necessarily lead to the degenerate eigenstates. Therefore, a special case where the DPs and EPs coexist with the same parameters may appear in non-Hermitian systems, and such coincidence of different kinds of degeneracies is called the hybrid diabolical-exceptional points (HPs).[94,106,121] In a recent experimental study of multimode bosonic system, the HPs have been harnessed to achieve resilient and robust mode switching,[122] while the on-demand mode switching can be impeded due to the breakdown of adiabaticity at multiple exceptional degeneracies.

3. APPLICATIONS OF QUANTUM EXCEPTIONAL POINTS IN NON-HERMITIAN SYSTEMS

3.1. Analogues Quantum Effect of HEPs. Though the EP is a radically new physical concept, its experimental demonstration and the counterintuitive aspects in quantum optoelectronic systems remain largely unexplored due to the difficulties of implementing the PT-symmetric non-Hermiticity, as well as the decoherence and dephasing that hinder the observation of the related effect in the quantum regime. Fortunately, the mathematical similarity between the single-particle Schrödinger equation and the Maxwell equations of the electromagnetic field offers a test bed for verifying the fundamental properties of non-Hermitian physics through the optical arrangement, where the refractive index of optical media $n(x)$ plays the role of potential function $V(x)$ in the single-particle Schrödinger equation. Its Hamiltonian becomes PT symmetric if the complex potential shows the feature of $V(x) = V^*(-x)$. Accordingly, this requirement of the potential function involved to achieve the PT symmetry is transferred into the restrictions imposed on the profile of complex dielectric permittivity; i.e., the imaginary and real parts of $n(x)$ are respectively odd and even symmetry about $x = 0$. Since the positive (negative) sign of the imaginary part of $n(x)$ indicates the attenuation (amplification) of light, the HEPs can be accessed by engineering the optical gain and loss in active photonic structures.[123,124] In this respect, the standard optical configurations are the coupled waveguides[125] and WGM microcavities,[126,127] where one features optical gain while another is lossy. The occurrence of a PT symmetry phase transition at an EP2 can be verified through the variation of spatial profiles of supermodes in the coupled photonic structures.

The success of implementing HEPs in non-Hermitian classical photonic systems has spurred plenty of research activities aimed to simulate the non-Hermitian physics of the EPs predicted by quantum theory, such as the phase transition between the PT-symmetry and PT-symmetry broken phases,[1,124] the chiral state transfer by encircling an EP,[8,128] and the $\epsilon^{1/k}$ relation of spectral splitting as the system with EPk subjected to perturbation ϵ.[101−103,129] These intriguing non-Hermitian features of the HEPs inspire the development of on-chip photonic devices with novel functionalities and advantageous performance. In this regard, the HEPs find important applications in achieving single-mode lasing in a high-Q WGM microcavity,[130,131] which supports multiple longitudinal modes with similar quality factors. It leads to a longstanding challenge of multimode emissions in micro- and nanolaser systems, which can lead to fluctuations and instability in the output. Traditional methods of suppressing the competing parasitic modes can be complex and may not be universally applicable. By introducing an additional passive cavity with an equal amount of loss, the PT symmetry can be established in the

https://doi.org/10.1021/acsnano.4c15648
ACS Nano XXXX, XXX, XXX−XXX

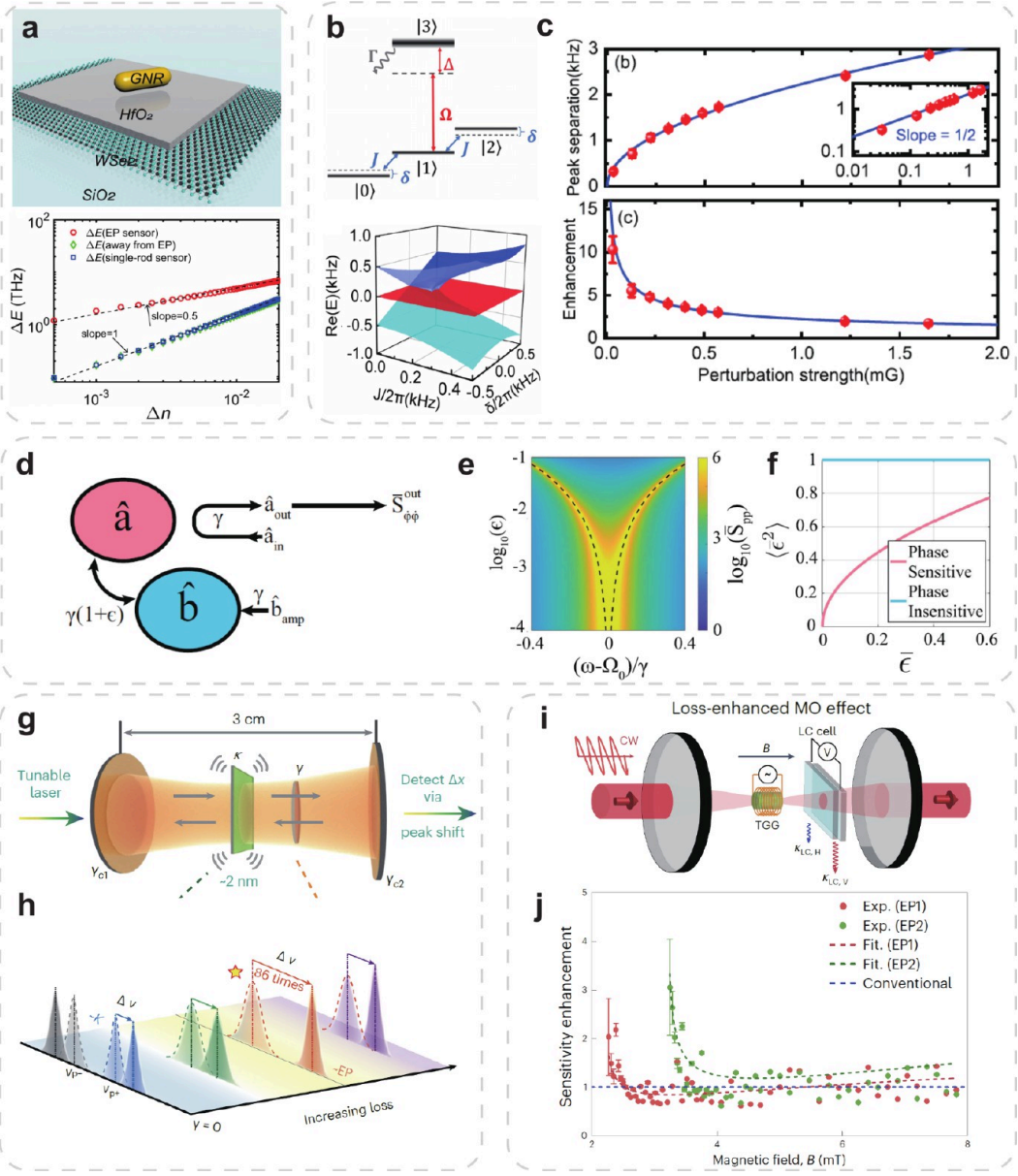

Figure 3. Quantum sensing based on quantum EPs. (a) The demonstration of ultrasensitive quantum sensing for a nanoscale environmental refractive index based on EP2s of a plasmon-exciton strong-coupling system.[139] Adapted with permission from ref 139. Copyright 2022 The Authors. Published by Chinese Laser Press and licensed under CC-BY 4.0. (b) Quantum EP-enhanced sensing of a magnetic field in thermal atoms ensembles. Atomic energy level diagrams and the real parts of the eigenvalues of corresponding effective Hamiltonian versus detuning δ and interaction strength J. (c) The measured optical polarization rotation and the corresponding enhancement with EP2.[57] Adapted with permission from ref 57. Copyright 2023 The Authors. Published by American Physical Society, licensed under CC-BY 4.0. (d) Schematic of PT-symmetric EP sensors used to detect a weak signal. Mode a is coupled to the output, while mode b is amplified and noisy. (e) The phase quadrature spectrum versus the distance to EP. (f) The ability of an EP sensor to estimate the value of small parameter (right).[72] Adapted with permission from ref 72. Copyright 2024 American Physical Society. (g) Schematics of a nanometric displacement detector consisting of a movable mirror in the center of the FP cavity. The insertion loss is provided by an Er^{3+}-doped quartz crystal. (h) Illustration of the loss-enabled nanometrology. The optimal case is near but not exactly at the EP.[150] Adapted with permission from ref 150. Copyright 2024 Springer Nature. (i) and (j) Schematics of experimental setups for the loss-enhanced magneto-optical effect and the corresponding sensitivity enhancement, respectively.[151] Adapted with permission from ref 151. Copyright 2025 Springer Nature.

coupled WGM microcavities. The asymmetric spatial profiles at the EP2 result in different lasing thresholds of supermodes, allowing for the single-mode operation with a suppression ratio exceeding 20 dB and offering superior performance in terms of efficiency. This strategy has alternative realizations of a single WGM microcavity with a transverse lasing mode of WGM microcavity,[132] electrically pumped microlasers.[133] The results show that the HEPs can facilitate the mode selectivity over a broad bandwidth without additional intricate components regardless of the spectral bandwidth of the gain materials.

On the other hand, the singular response of the EPs enabled by the coalesced eigenstates can be harnessed to enhance the sensitivity of optical sensing through the spectral splitting. The chiral EPs can be introduced in the WGM microtoroid by employing two nanoscale scatterers to precisely tune the coupling between a pair of degenerate WGM cavity modes.[103]

https://doi.org/10.1021/acsnano.4c15648
ACS Nano XXXX, XXX, XXX−XXX

When a target nanoscale object, such as a nanoparticle, enters the evanescent field of the cavity, it perturbs the system away from the chiral EPs and leads to spectral splitting. The sensitivity is significantly enhanced due to the square-root topology near the EP2s, and hence, the frequency splitting scales as the square root of the perturbation strength, in stark contrast to the linear scaling observed in traditional sensing schemes. In another setup of an EP-based sensor, a coupled three cavities arrangement with a tailored gain−loss distribution was proposed, which exhibits an EP3 and follows a cube-root dependence on induced perturbations in a refractive index.[102]

A gyroscope is another kind of optical sensor that has important applications in the scenarios of navigation, positioning, and attitude sensing. The Sagnac effect is a fundamental principle in gyroscopes, which is typically linearly proportional to the rotational velocity. In ring laser gyroscopes, EP2 can be induced by introducing a differential loss contrast between the counter-propagating lasing modes and balancing the modes coupling. This configuration results in a square-root dependence of the Sagnac scale factor on the rotational velocity, with a substantial enhancement up to 20 times greater than that of traditional ring laser gyroscopes.[134] In another configuration of laser gyroscopes based on the stimulated Brillouin lasing in the WGM microcavity, the EP2 can be established by the precise control of Brillouin-induced dispersion to create the eigenstates coalescence of two dissipatively coupled counter-propagating WGM modes.[135] The Sagnac effect induces opposing frequency shifts between the WGM modes and is monitored through the dual-SBL beating frequency, where a 4-fold increase in the Sagnac scale factor is observed by directly measuring rotations applied to the cavity. These studies show that the sensitivity enhancement at an EP is dependent on neither the materials nor the geometries of EP-based photonic sensors; instead, it emerges from the intrinsic properties of EPs, and thus can be applied to various photonic configurations and lead to a new class of on-chip sensors with unprecedented sensitivity.

As shown in a study of coupled waveguides,[136] a non-Hermitian system without gain can exhibit the hidden PT symmetry by performing a gauge transformation that factors out a global damping in the eigenstates. It indicates the existence of the HEPs in a wide class of passive non-Hermitian systems and extends the applicability of the exotic HEPs effects in developing the novel photonic devices.[137,138]

3.2. Recent Advances in EP-Based Sensors. *3.2.1. From Classical to Quantum Sensing near EPs.* Given the huge success of the HEPs in achieving ultrasensitive optical sensors at nanoscale, an intense research effort has been paid to explore the possibilities of enhancing the sensitivity of quantum sensing based upon the quantum EPs. Figure 3a shows a theoretical scheme based on a quantum system of strong plasmon-exciton coupling between the Au nanorod and WSe_2, which has demonstrated the enhanced sensitivity of spectral splitting induced by the perturbations in the refractive index at an EP2, with the similar characteristic of EP sensors in the classical optical regime.[139] The proposed model is operated at room temperature and thus holds potential for an experimental demonstration of the EP-enhanced quantum sensing, despite the metallic nanoparticles featuring high dissipation. By analyzing the generalized signal-to-noise ratio (SNR) of fluorescence spectra, Kuo et al. showed that the EP2 induced by a collection of quantum emitters strongly coupled to metallic nanoparticles is easier to observe due to the narrower line width of peak compared to the case of single quantum emitter.[140] The line width narrowing is a result of the smaller critical coupling strength for the EP2, which reduces the dissipation induced by higher-order plasmonic modes. In terms of experimental progress, a quantum realm of the EP-enhanced sensor with heterodyne detection has been achieved in a setup consisting of coupled active and passive optical modes.[141] The full eigenenergies spectrum obtained through the weak measurement reveals that a transition from the unbroken to the broken region of the PT symmetry occurred in the system. By introducing the perturbation on the frequencies of both modes, the frequency splitting of the system demonstrates an approximately nine times enhancement of sensitivity compared to a conventional Hermitian sensor. The EP-enhanced quantum sensing has also been demonstrated in thermal atomic ensembles, where the employed laser field couples with different energy levels creating unbalanced effective decay rates.[57] As shown in Figure 3b, the resultant effective non-Hermitian Hamiltonian is in a similar form of the anti-PT-symmetric system and can exhibit an EP2. A scheme of optical polarization rotation measurement was developed to capitalize on both the absorption and dispersion properties of the system, from which the enhanced sensitivity of the magnetic field by an order of magnitude was observed at the EP2; see Figure 3c.

3.2.2. Criticisms of Enhanced Sensitivity near Quantum EPs. Although many studies have demonstrated that the EPs can produce large sensitivity to the quantity (e.g., the spectral splitting) being sensed, the controversy over the enhanced performance of EP sensors has been ongoing for many years.[51,69−72,142−144] The controversy arises because in the parameter estimation the performance of a sensor should be defined by its precision, which is characterized by the signal-to-noise ratio (SNR) dependent on both the sensitivity and additional noise. Therefore, just the large sensitivity is not an adequate measure to assess the precision of the EP sensors since it does not necessarily lead to better SNR.[70] In practice, there exists a variety of additional noises in the experimental settings, such as the electronic noise of instruments, thermal noise for frequency fluctuation, and quantum noise from either an applied laser field or critical fluctuation near the lasing threshold, which can also be enhanced by the EPs. As a result, the measured parameters are accompanied by the increased uncertainty near the EPs.[69,70,143−147] In this respect, the studies of the PT-symmetric coupled two-mode system have proven that the SNR of this exemplary EP sensor cannot be improved due to the existence of inevitable quantum frequency noise near the EPs[72,144] (see Figure 3d and e). This conclusion is consistent with the theory of parameter estimation using the quantum Fisher information (QFI),[143,147] which is a measure of how well a quantum state can be used to estimate an unknown parameter and determines the upper bound of SNR. The results indicate that even below the lasing threshold, the excitation of all coalescent eigenstates counteracts the divergent susceptibility of eigenenergies, giving rise to smooth QFI at the EPs. The prediction has been validated by an experimental study of a laser gyroscope operated near an EP2, where the improved responsivity is precisely compensated by the increased laser noise.[148] Especially, a theoretical analysis based on the effective differential equation of mean time-evolution operator has shown that the presence of noise will inevitably lead to the exponential divergence of any initial state,

https://doi.org/10.1021/acsnano.4c15648
ACS Nano XXXX, XXX, XXX−XXX

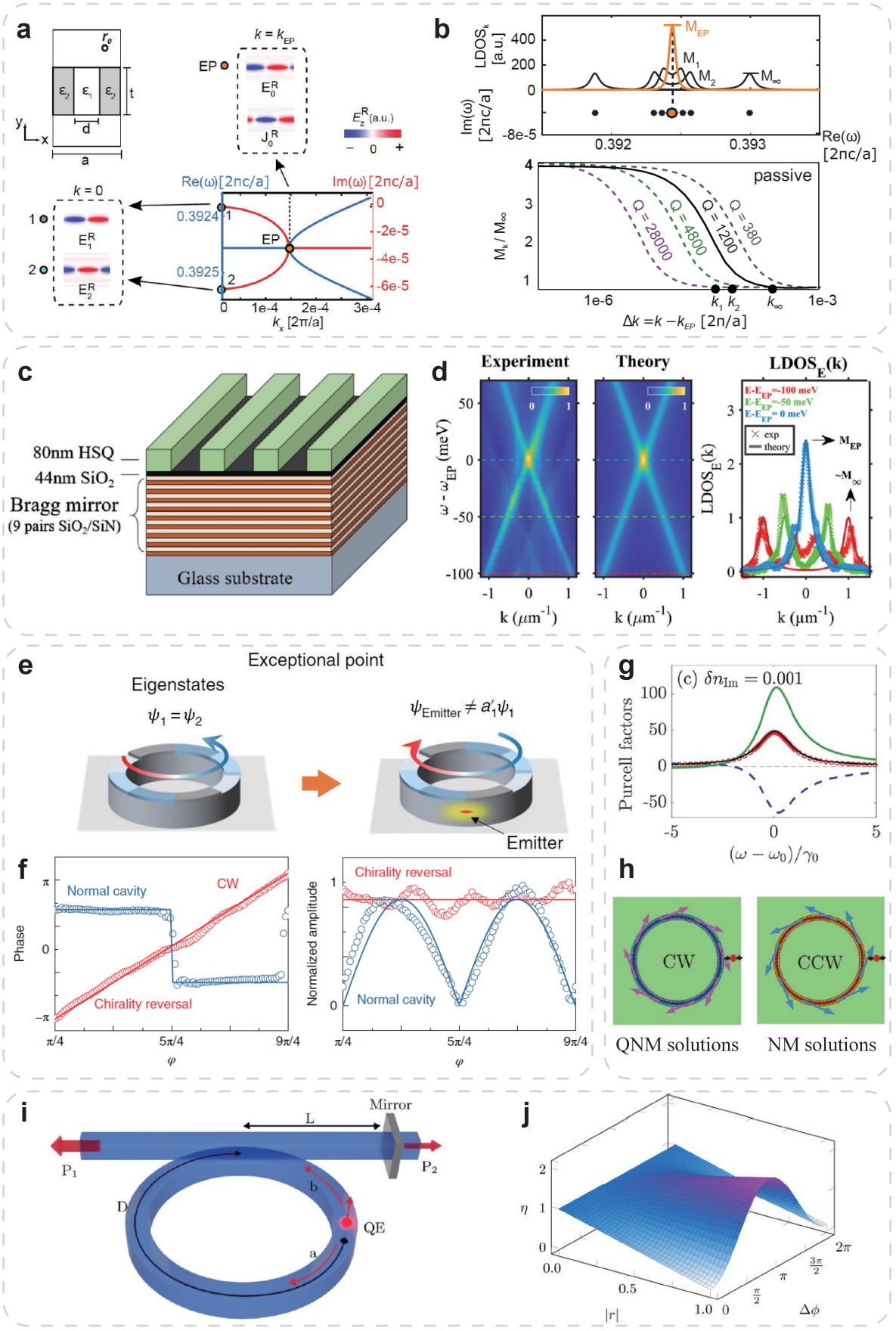

Figure 4. Modified spontaneous emission by EPs. (a) Passive periodic waveguides with EP2s. (b) LDOS for four *k*-values versus complex eigenfreuqencies of resonances (top) and the normalized LDOS peak for four structures with different *Q* values (bottom).[114] Adapted with

https://doi.org/10.1021/acsnano.4c15648
ACS Nano XXXX, XXX, XXX−XXX

Figure 4. continued

permission from ref 114. Copyright 2017 The Authors. Published by Optical Society of America and licensed under CC-BY 4.0. (c) Sketch of the passive sample composed of a hydrogen silsesquioxane (HSQ) grating on top of a Bragg mirror with a 44 nm spacing layer of SiO_2. (d) Experimental (left) and theoretical (middle) LDOS maps extracted from the photoluminescence measurements of the active sample. Three horizontal isofrequency cross sections of LDOS are shown in the right panel.[38] Adapted with permission from ref 38. Copyright 2022 American Physical Society. (e) Schematic of a ring cavity operating at an exceptional point, where the two eigenstates coalesce (left). A single emitter can become fully decoupled from the coalesced eigenstate and radiate to the missing dimension with opposite handedness (right). (f) Phase and amplitude of the single-emitter radiation field as a function of φ.[34] Adapted with permission from ref 34. Copyright 2020 Springer Nature. (g) Classical Purcell factor of ring resonators in (e) with the refractive index difference $\delta n_{\mathrm{Im}} = 0.001$ and the quasi-normal mode (QNM) decomposition. (h) Power flow from QNM and normal mode solutions.[165] Adapted from ref 165. Copyright 2022 American Chemical Society. (i) Schematic of a microring resonator for implementing CEP with a quantum emitter located inside the resonator. (j) Purcell factor enhancement at chiral EP2s as a function of the mirror field reflectivity amplitude |r| and propagating phase of light in waveguide $\Delta\phi$.[35] Adapted with permission from ref 35. Copyright 2021 The Authors. Published by American Physical Society, licensed under CC-BY 4.0.

which occurs at a time scale depending on the noise amplitude.[149] This implies that the continuous operation of a sensor near the EPs is quite demanding. Therefore, the design of a sensor operated at quantum EPs might face the challenges of not only the quantum-noise limit but also the problem of stabilization.

3.2.3. Toward the Improved SNR with Noise. From the perspective of quantum information, the sensitivity enhancement means the supplement of extra quantum resources accompanied by the postselection for parameter estimation. A similar conclusion can be also drawn from the analysis of the quantum EP sensors based on spin systems: the improved sensitivity at the EPs is offset by the enhanced uncertainty, and thus the ultimate precision of practical sensors is bound by the uncertainty, i.e., the limited quantum resources.[71] It indicates that the performance of non-Hermitian sensors cannot surpass their Hermitian counterparts, but also implies the possible routes for improving SNR. For linear quantum sensors in the standard PT symmetric configuration of coupled two modes, the genuine improvement of the SNR at the EPs can be achieved by implementing a phase-sensitive gain, such as an optical parametric amplifier, and then the imprecision of the EP sensors will demonstrate the desirable $\sqrt{\varepsilon}$ dependence (see Figure 3f).[72] Recent studies have also shown that the improvement of the SNR at an EP is achievable if the role of an external laser source is taken into account: The QFI at EPs diverges when at least one photonic mode reaches the lasing threshold, suggesting that the EPs do not inherently offer a sensing advantage, but can improve the sensitivity when combined with the lasing occurring in the PT-symmetric systems at the expense of extra energy consumption.[51,69,145,152] This is also valid in a nonlinear regime, where a few studies reported the enhanced SNR of the EP-based sensors.[153−155] Remarkably, a recent study has shown that the noise can be utilized to improve the SNR of a nonlinear cavity system exhibiting bistability, where the bistable mode switching can be driven by the presence of noise in temporal frequency modulation.[156] In addition, in an experiment of a displacement sensor simply based on a Fabry−Pérot (FP) optical cavity with a movable object placed at the center (see Figure 3g), the maximum of 5-fold SNR enhancement has been observed at the transmission peak degeneracy near the EP, accompanied by 2 nm resolution and 86 times improvement compared to the Hermitian counterpart (see Figure 3f).[150] Very recently, the 3-fold improvement of the precision of an EP magnetic sensor has also been reported in the setup of a Faraday FP cavity, where an EP2 is introduced by the loss difference of two polarized modes through a liquid crystal (see Figure 3i−j).[151] On the other hand, as the SNR of any reciprocal system including the EP sensors is constrained by a fundamental bound involving the average intramode photon number, the nonreciprocity becomes an important resource to break the bound of SNR.[148] It is worth noting that a two-site system with unidirectional coupling corresponding to the special case of CEP thus recovers the $\sqrt{\varepsilon}$ splitting dependence.

The research effort to clarify the impact of additional noises on the sensitivity enhancement opens up a new horizon for understanding and breaking the fundamental sensitivity limit of quantum sensors operated at the EP. Further experimental verification along this direction is of great importance and can facilitate the development of quantum sensors with superior performance.

3.3. Modified Spontaneous Emission by EPs. Spontaneous emission (SE) results from the interaction of an excited quantum emitter (QE) with the quantized electromagnetic field of its surrounding environment.[157] The concept of the SE is at the heart of quantum optics, but also determines the performance of many optoelectronic elements, ranging from the macroscopic devices for lighting and displays, to the fundamental physical processes related to light emission and absorption, such as nanolasers[158] and quantum light sources[33,159] at nanoscale. Understanding the modification of the SE at the EPs is of great importance to reveal the quantum effect of the EPs and advance nanophotonic applications.

As found by Purcell, the SE can be controlled by engineering the electromagnetic environment of a QE.[160] The modified emission rate of a QE in the excited state is determined by the electromagnetic local density of states (LDOS), which defines the number of available electromagnetic modes for QE to decay.[157,161−163] Therefore, the non-Lorentzian cavity response at the EPs can dramatically modify the SE of a QE. The traditional nondegenerate perturbation theory of the SE is invalid at the EPs since it yields the infinite enhancement factor due to the divergence of the Petermann factor, a measure of mode nonorthogonality. A modified Jordan-form-based perturbation theory proposed by Pick et al. can derive finite bounds on the enhancement at the EPs.[114] It predicts a maximum of four times enhancement of LDOS at the EP2, which was demonstrated in a passive one-dimensional waveguide structure with periodic index modulation, as shown in Figure 4a. An EP2 can be formed by tuning the wavevector and the permittivity contrast, where two eigenmodes merge into a single degenerate mode. The 4-fold enhancement of the LDOS was found regardless of the quality factor of the structure since the spectrally integrated LDOS is a constant (see Figure 4b). They also proposed a three-

https://doi.org/10.1021/acsnano.4c15648
ACS Nano XXXX, XXX, XXX−XXX

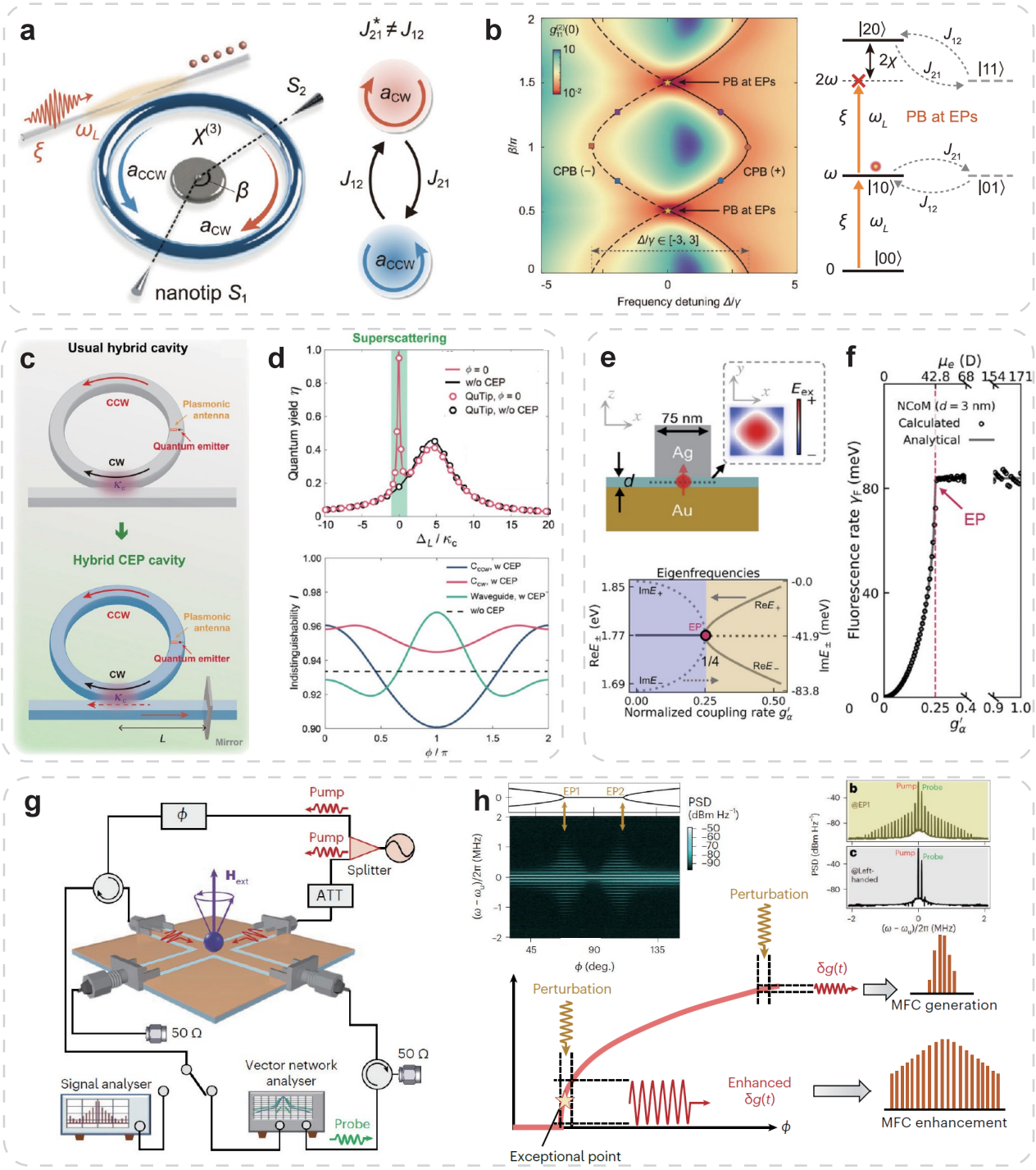

Figure 5. Nonclassical light generation with EPs. (a) and (b) Single-photon blockade at periodic EPs in a microring resonator with strong Kerr nonlinearity $\chi^{(3)}$ driven by a laser field.[33] Adapted with permission from ref 33. Copyright 2022 Wiley-VCH GmbH. (c) Schematic diagram of the hybrid CEP cavity based on the WGM cavity, which supports the degenerate clockwise (CW) and counterclockwise (CCW) modes with unidirectional coupling provided by the mirror, which is different from the usual hybrid cavity without chiral EP. κ_c is the decay of WGM modes induced by waveguide and L is the distance between the cavity-waveguide junction and the mirror. (d) The occurrence of superscattering (upper panel) and the indistinguishability of single-photon generation (lower panel) at chiral EP.[40] Adapted with permission from ref 40. Copyright 2024 The Authors. Published by Springer Nature, licensed under CC-BY 4.0. (e) Schematic of a nanoparticle-on-mirror plasmonic cavity with a QE positioned at the center of the gap. The excited field distribution is within the xy plane, and the isolated EP2 appears with $g_a' = g_a/\kappa_a = 0.25$. (f) The fluorescence rates as a function of the normalized coupling rate g_a'.[159] Adapted with permission from ref 159. Copyright 2024 The Authors. Published by American Institute of Physics, licensed under CC-BY 4.0. (g) Experimental setup of coupled pump-induced magnon mode (PIM) and Kittel mode (KM). (h) Schematic diagram of magnon frequency comb (MFC) generation and enhancement. A perturbation from the probe leads to nonlinear PIM−KM coupling and produces the densest MFC near the two EP2s.[47] Adapted with permission from ref 47. Copyright 2024 Springer Nature.

https://doi.org/10.1021/acsnano.4c15648
ACS Nano XXXX, XXX, XXX−XXX

dimensional photonic crystal structure with higher-order Dirac points through the inverse design,[37] where an EP3 can be induced by accidental third-order degeneracy at the Γ point involving the monopolar, dipolar, and quadrupolar modes. The LDOS was shown to exhibit an 8-fold enhancement at the EP3, consistent with the theoretical prediction. However, the fabrication of the proposed structures proved challenging at the optical band with current technologies. A few years later, the first experimental demonstration of the SE enhancement at an EP3 has been achieved in photonic crystal slabs embedded with high-quantum-yield active material of perovskite colloidal nanocrystals.[38] As shown in Figure 4c and d, the EP3 is directly observed from the angle-resolved reflectivity measurements, and the corresponding LDOS enhancement is revealed through the photoluminescence signal of active material. The LDOS manifests 2.56 times enhancement at the EP3, which remains finite and shows good agreement with the theoretical value. Besides modifying the SE rate, the EPs can also render the SE dynamics. By coupling the QE to one-dimensional continuum with a van Hove singularity at the band edge, Garmon et al. found the formation of anomalous-order EP2 with a QE near the band edge, which is signified by the enhanced SE rate accompanied by an unusual form of $1 - Ct^{3/2}$ during the key time scale of the decay process.[164] The result indicates the intriguing quantum physics arising from the interplay between the photonic band edge and EPs.

Though the LDOS enhancement is in general related to the temporal dynamics of the SE, recent studies have shown that the chiral EP (EP2s) can also exhibit a significant impact on the emission patterns of a QE. In an experimental work of Chen et al., a chiral EP is implemented in a ring cavity between two counter-propagating WGM modes through the periodic refractive index modulation along the azimuthal direction,[34] in a similar configuration that has been used to build a single-mode lasing nanolaser[131] (see Figure 4e). The coalesced eigenstates at EP2s mean that either the counterclockwise (CCW) mode or the clockwise (CW) mode survived in the CEP cavity. A surprising phenomenon emerges by placing a linearly polarized QE in a special location of the cavity where the unidirectional coupling strength between two WGM modes is equal to the loss of them. In this case, the coupled-mode theory indicates that the QE will excite the missing eigenstate instead of the survived one. The predicted phenomenon of CEP cavity has been experimentally confirmed in both the electromagnetic and acoustic systems, where the amplitude and phase of radiating field exhibits essential different properties from that of normal cavity without the chiral EP, as shown in Figure 4f. Since the CCW and CW modes feature the opposite chirality, this exotic QED behavior is called the chirality-reversal radiation and is explained by the coupled-mode theory as a result of destructive interference between the directly radiated and the backscattered waves. Due to the openness of WGM cavity, the quasi-normal mode (QNM) theory is a more rigorous approach than the normal mode to describe the interaction with a dipole QE, where the amplification and dissipation of a cavity mode are naturally captured by the complex eigenfrequency of QNM.[165,166] The QNM analysis indicates that the chirality-reversal radiation originates from two main QNM modes in the CEP cavity related to the experiment, as Figure 4g and h, providing a different interpretation of the chiral power flow from a linearly polarized dipole at EPs.

Based on the quantized pseudomode theory, the quantum dynamics of a QE in the CEP cavity can be well described by the Lindblad master equation with a two-mode Jaynes–Cummings Hamiltonian, and then the LDOS can be analytically obtained.[35,98,114] The LDOS of the CEP cavity manifests a non-Lorentzian line shape due to the additional squared-Lorentzian term contributed by the EP2s. For the configuration of the CEP cavity shown in Figure 4i, the LDOS can be feasibly tuned from enhanced to completely suppressed by adjusting the location of the mirror, which controls the phase of coupling strength between two WGM modes. Accordingly, the decoherence suppression of strong QE-cavity coupling and the bound dressed states can be achieved at the chiral EP, which will be beneficial to applications of quantum information processing and quantum computing.[98] The numerical simulation has shown that the suppression of the SE results from the decoupling of the QE from the eigenmode of the CEP cavity.[35] These findings exhibit the great ability of the chiral EP in controlling the SE of the QE. Beyond the linear Purcell effect, the EPs can also enhance the interaction between a QE and a nonlinear cavity. Pick et al. has shown that an EP2 in $\chi^{(2)}$ cavity can enhance the frequency up-conversion process by over 2 orders of magnitude compared to that without an EP2, enabling the high-efficiency nonlinear light generation for third-harmonic generation, four-wave mixing, and two-photon down-conversion.[167]

3.4. Nonclassical Light Generation with EPs. Classical light from thermal and coherent sources features bunched and uncorrelated photons, respectively. Nonclassical light sources with sub-Poisson photon statistics (antibunched photon), especially the single-photon sources, demonstrate the quantized nature of the electromagnetic field and find important applications in quantum information processing, quantum communication, and quantum cryptography. The effect of a single-photon blockade (1PB),[168,169] a physical process that the absorption of the first photon blocks the absorption of subsequent one, can be utilized to create strong photon correlations and develop single-photon devices in diverse quantum systems. While several mechanisms have been found for 1PB, the typical physical realizations require quantum systems with nonlinear spacing of energy levels in the single- and two-excitation Hilbert subspaces. Since the EPs correspond to the coalescence of both eigenenergies and the associated eigenstates, they can be harnessed to control the quantum correlations of photons emitted by a quantum system.

In the context of tuning photon correlations by the EPs, Huang et al. revealed the generation of high-purity single photons at the chiral EPs in a $\chi^{(3)}$ WGM cavity.[33] The chiral EPs are introduced through the unidirectional coupling between the CCW and CW modes, which is induced by two nanotips in the vicinity of the cavity; see Figure 5a for illustration. In this configuration, the parameters of the HEPs are found to coincide with LEPs by inspecting the cavity excitation spectrum. As Figure 5b shows, the chiral EPs suppress the transition from the two-photon state $|11\rangle$ to another two-photon state $|20\rangle$. On the other hand, the Kerr interaction of the nonlinear cavity shifts the energy of the two-photon state $|20\rangle$ by 2χ from the resonant excitation of single-photon states with energy ω. These two factors together prevent the excitation of two-photon states $|20\rangle$ in the stationary limit, leading to the occurrence of 1PB in one of the WGM modes. By changing the relative angular position

https://doi.org/10.1021/acsnano.4c15648
ACS Nano XXXX, XXX, XXX−XXX

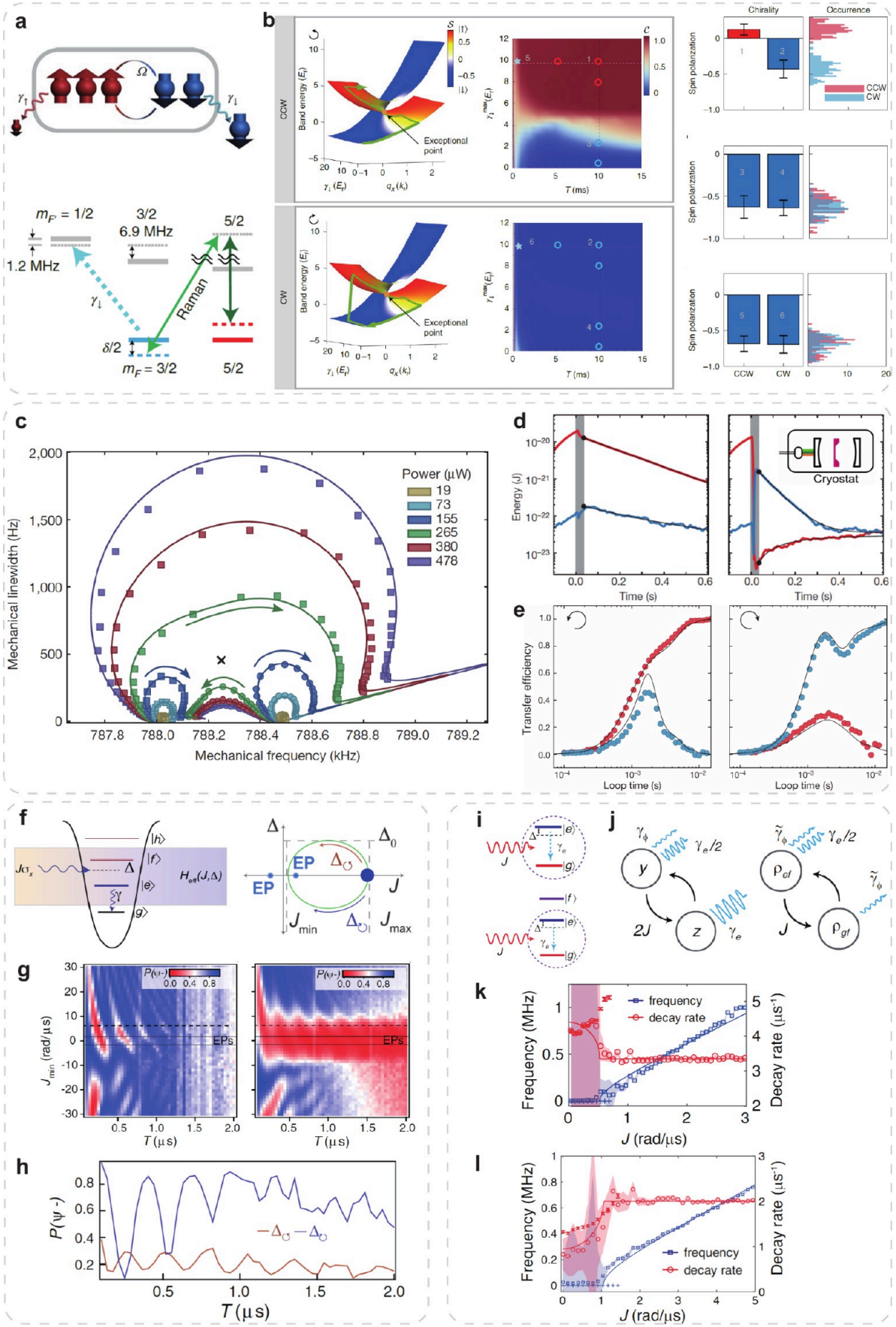

Figure 6. Quantum state control by EPs. (a) Sketch of ultracold Fermions with two spin states coupled by Raman beams. (b) Topological chiral spin transfer by dynamically encircling an EP by tuning the loss and two-photon detuning. The results show the chiral behavior of the

https://doi.org/10.1021/acsnano.4c15648
ACS Nano XXXX, XXX, XXX−XXX

Figure 6. continued

final spin polarization (1−4), while no chirality is observed when dynamic encircling is instantaneous (5 and 6).[25] Adapted with permission from ref 25. Copyright 2022 Springer Nature. (c) The complex eigenvalues of the normal modes of the membrane in a cavity excited by a laser. (d, e) Topological energy transfer in these two modes, where the resultant intracavity field drives the vibrations of the membrane via radiation pressure. The energies of modes as a function of time are shown in (d), where the gray shaded region indicates the time during which the control loop is implemented. The control loop can enclose the EP (right) or not (left). The transfer efficiency versus the duration of the control loop is plotted in (e).[8] Adapted with permission from ref 8. Copyright 2016 Springer Nature. (f) The energy states of the transmon circuit with the non-Hermitian qubit and the direction of parameter sweep. (g) The eigenstate population after one period evolution for two sweep directions and two cuts (h).[62] Adapted with permission from ref 62. Copyright 2021 American Physical Society. (i) Schematic of a driven dissipative qubit and a driven dissipative qutrit. (j) The coupling between the Pauli expectation values y and z with different losses can be viewed in terms of a two-mode system (y and z) with passive PT symmetry and EPs (left), while the coupling between two coherences of the density matrix ρ_{ef} and ρ_{gf} that experience unbalanced losses produces Liouvillian EP. Panels (k) and (l) show the respective oscillation frequency and decay rate at different drive amplitudes, where the transition marks an LEP.[32] Adapted with permission from ref 32. Copyright 2022 American Physical Society.

between two nanotips, the chiral EPs appear periodically, leading to significant variation of photon statistics from strongly bunched photons ($g^{(2)}(0) \approx 10$) to high-purity single photons ($g^{(2)}(0) \approx 0.01$). The EPs not only impact the steady-state properties of a quantum system, but also render the quantum dynamics. By constructing the LEP in a nonlinear cavity, Geng et al. demonstrated the dynamical 1PB with dual pumps.[170] In this configuration, the 1PB occurs at the LEP through the interference of different paths during the two-photon excitation process, which depends on the amplitude and frequency detuning of the excitation fields. As a result, periodic single-photon generation can be achieved with an adjustable frequency.

While the 1PB in the WGM microcavity generally demands a cryogenic environment due to the relatively weak light-matter interaction, the integration of plasmonic structures to form a hybrid plasmon-photon microcavity allows quantum-optical applications at room temperature. As shown in Figure 5c and d, a recent study has found that such hybrid microcavity can generate indistinguishable single photons at room temperature without the aid of the 1PB. Instead, it is achieved by enhancing the quantum yield through the superscattering occurring at the chiral EPs.[40] In previous studies, the schemes of room-temperature single-photon sources have also been proposed based on the microcavity but suffer from the slow emission rate.[171,172] Plasmonic structures can enhance the fluorescence rate of the QE-based single-photon sources due to the strong electric field enhancement, with a typical value larger than 100 GHz. As shown in Figure 5e and f, the study of Zhou et al., the fluorescence rate under the weak-coupling regime is enhanced with increased plasmon-QE coupling strength and reaches the maximum of about 10 THz at EP.[159] Further increasing the coupling strength will not produce a faster fluorescence rate but instead lead to the quenching of single-photon emission. Though conducted in a special plasmonic structure, the study reveals the existence of a quantum limit to the performance of single-photon devices related to the EPs.

Another kind of useful nonclassical light source is the frequency combs, which can be a quantum resource for generating heralded single photons and energy-time entangled pairs and plays an important role in applications of precision spectroscopy, ultrasensitive detection, and atomic clocks due to their high time−frequency accuracy. The frequency combs are generated through nonlinear interactions, which can be notably enhanced by the EPs, but remain unexplored in experiments. Very recently, Wang et al. finished the first experimental demonstration of the EP-enhanced frequency combs in the magnon system.[47] As Figure 5g shows, the setup is based on a coupled system consisting of a pump-induced magnon mode (PIM) and a Kittel mode (KM) in a magnetic insulator. The EP2s are constructed by the precise control of the PIM-KM coupling strength through the inherited chirality of PIM induced by a magnetic field. Furthermore, EP2s are extended to an exceptional line in the higher-dimensional parameter space by incorporating pump power as an additional control parameter. As shown in Figure 5h, the extension of the EP2s offers great convenience for optimizing the performance and results in the generation of dense magnon frequency combs with a record number of teeth over 32 and broadening of the frequency band, setting a new benchmark in the field.

3.5. Quantum States Controlled by EPs and Related Applications. As branch-point singularities in the parameter space, the EPs play an important role in determining the states of a quantum system in both the dynamical evolution and stationary limit. An interesting dynamical quantum effect related to the EP singularities is the chiral state transfer, where the final state after the adiabatic evolution of encircling an EP cannot recover the original state with a single loop, in stark contrast to the adiabatic evolution of accidental degeneracies in the Hermitian systems. This phenomenon is linked to the nontrivial topological features of the EPs and has been demonstrated as the chiral mode conversion in microwave waveguide system.[128]

In the quantum regime, the chiral state transfer has been demonstrated in a many-particle quantum system consisting of ultracold Fermions ^{173}Yb.[25] The synthetic spin−orbit coupling is created between two hyperfine states within an engineered energy band coupled by Raman transition beams, as shown in Figure 6a. By adjusting the spin-dependent atom loss, a tunable non-Hermitian Hamiltonian is realized and manipulated to create an EP2; see Figure 6b. The chiral property of the EP is revealed by dynamically encircling it in the parameter space, demonstrating the transferred chirality of atom spin due to the breakdown of adiabaticity. Based on the same principle, the energy transfer by encircling an EP has also been demonstrated in an optomechanical system.[8] In this setup, the coupling between two mechanical modes of the membrane inside a cavity can be controlled to form an EP2 by applying a laser field. The frequency and power of the laser were varied to sweep out a closed rectangular loop around the EP. This topological operation results in the energy transfer from one mode to another, and this transfer is nonreciprocal, depending on the direction of the loop, as shown in Figure 6c and d. Besides these two examples, similar phenomena of the chiral state transfer have been observed in the diverse quantum systems, such as a single NV center,[55,173,174] exciton-polariton

https://doi.org/10.1021/acsnano.4c15648
ACS Nano XXXX, XXX, XXX−XXX

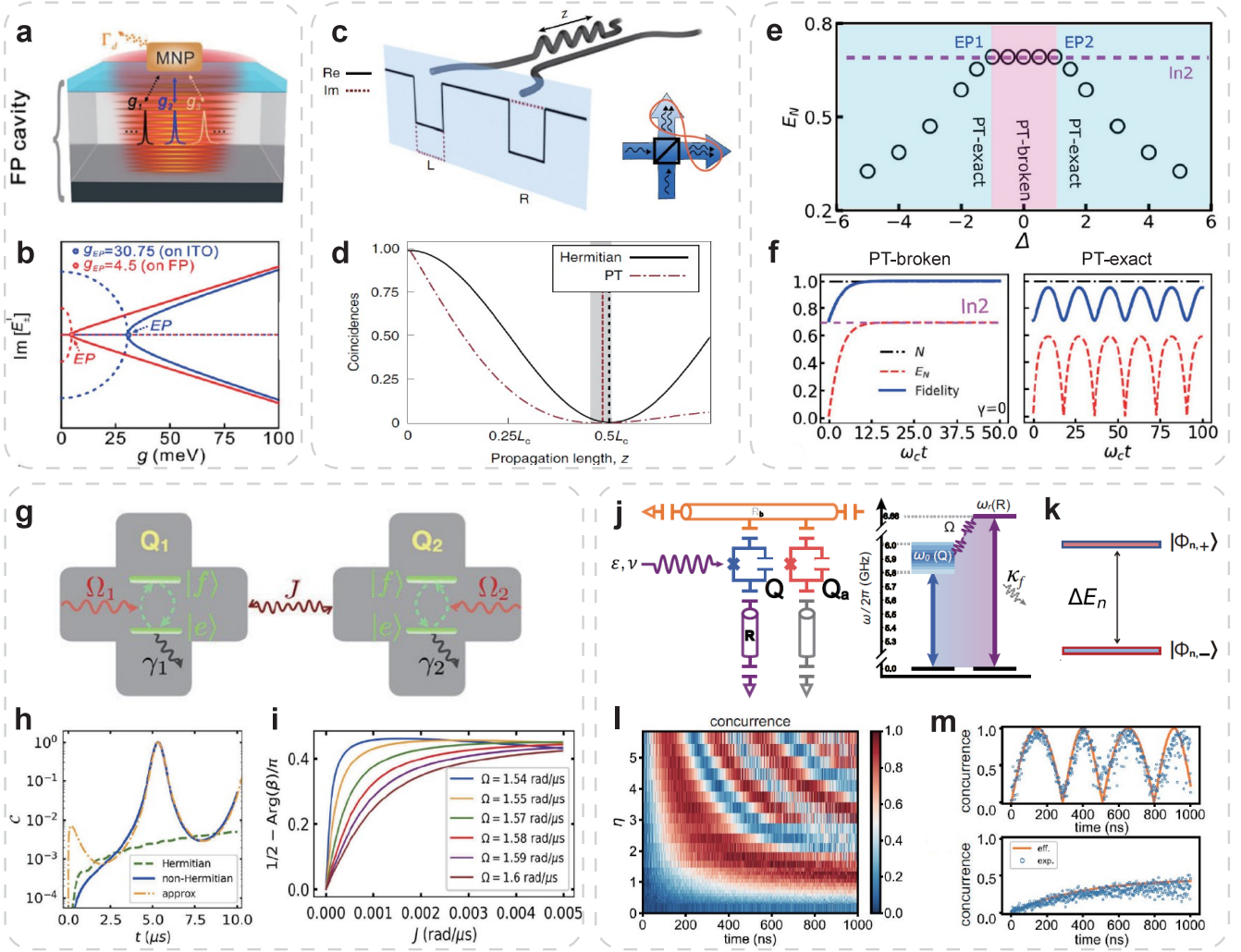

Figure 7. EP-empowered quantum state control for quantum-optical applications. (a) Schematics of a metal nanoparticle (MNP) residing in the microcavity-engineered electromagnetic environment. (b) Real (solid curves) and imaginary (dashed curves) parts of the eigenenergies versus coupling strength at resonance.[42] Adapted with permission from ref 42. Copyright 2023 American Physical Society. (c) Implementation of passive PT symmetry in a coupled two-waveguide system via a symmetric refractive index distribution and an asymmetric loss distribution. Two indistinguishable photons are launched into the two waveguides. (d) The analytical solution for the coincidence rate shows a HOM dip. In the lossy PT-symmetric case, the bunching occurs after a shorter propagation length.[30] Adapted with permission from ref 30. Copyright 2019 Springer Nature. (e) Level attraction of the cavity magnon system. Solid and dashed lines represent the real and imaginary parts of the eigenvalues, respectively. (f) Time evolution of particle number and entanglement measure under resonance with broken (left) and exact (right) PT symmetry.[180] Adapted with permission from ref 180. Copyright 2020 American Physical Society. (g) Schematic of two coupled non-Hermitian qubits with an external drive. (h) The corresponding concurrence evolution near the fourth-order EP. (i) Phase of coefficient β of quantum state $|fe\rangle$ relative to the corresponding value for $J = 0$ at different Ω. The increased slope on approaching the EP at $\Omega = 1.5$ rad/μs indicates the enhancement due to proximity to the EP2.[28] Adapted with permission from ref 28. Copyright 2023 American Physical Society. (j) Physical implementation of a superconducting qubit Q highly detuned from a lossy resonator R. The Q-R interaction is enabled with an ac flux, which modulates Q's energy gap around the mean value ω_0, with a frequency ν mediating a photonic swapping coupling at one sideband, with the coupling strength controlled by the modulating amplitude ε. (k) The system dynamics can be cast onto different $U(1)$-symmetric eigenspaces, where there exists two eigenstates $|\Phi_{n,\pm}\rangle$ separated by a gap of ΔE_n. (l) Evolutions of the concurrences for different values of η. (m) Complementary evolutions for $\eta = 5$ (upper panel) and 0.5 (lower panel). The orange solid curves are the numerical simulations based on the effective Hamiltonian, while the blue circles are the experimental results.[78] Adapted with permission from ref 78. Copyright 2023 American Physical Society.

systems,[26] quantum walk,[175] and superconducting circuit.[32,62,176] It is worth noting that as demonstrated both theoretically and experimentally in quantum walk,[175] the evolutionary state around the ELs is independent of the initial state and evolution direction, and thus the resultant quantum state transfer is more efficient than the case of encircling the EPs. In particular, the chiral state transfer by encircling an EP in the study of the superconducting circuit is verified through the quantum dynamics of the final state,[176] which clearly demonstrates the quantum coherence related to the complex energy landscape, as shown in Figure 6e–g. This strategy provides a general method to unveil the change of quantum nature of a state after encircling the LEPs, which may be different from the HEPs if the system is nonequilibrium or the EPs are induced by the decoherence and quantum jump[32,62] (see Figure 6h–k for instance) and hence does not admit the

https://doi.org/10.1021/acsnano.4c15648
ACS Nano XXXX, XXX, XXX−XXX

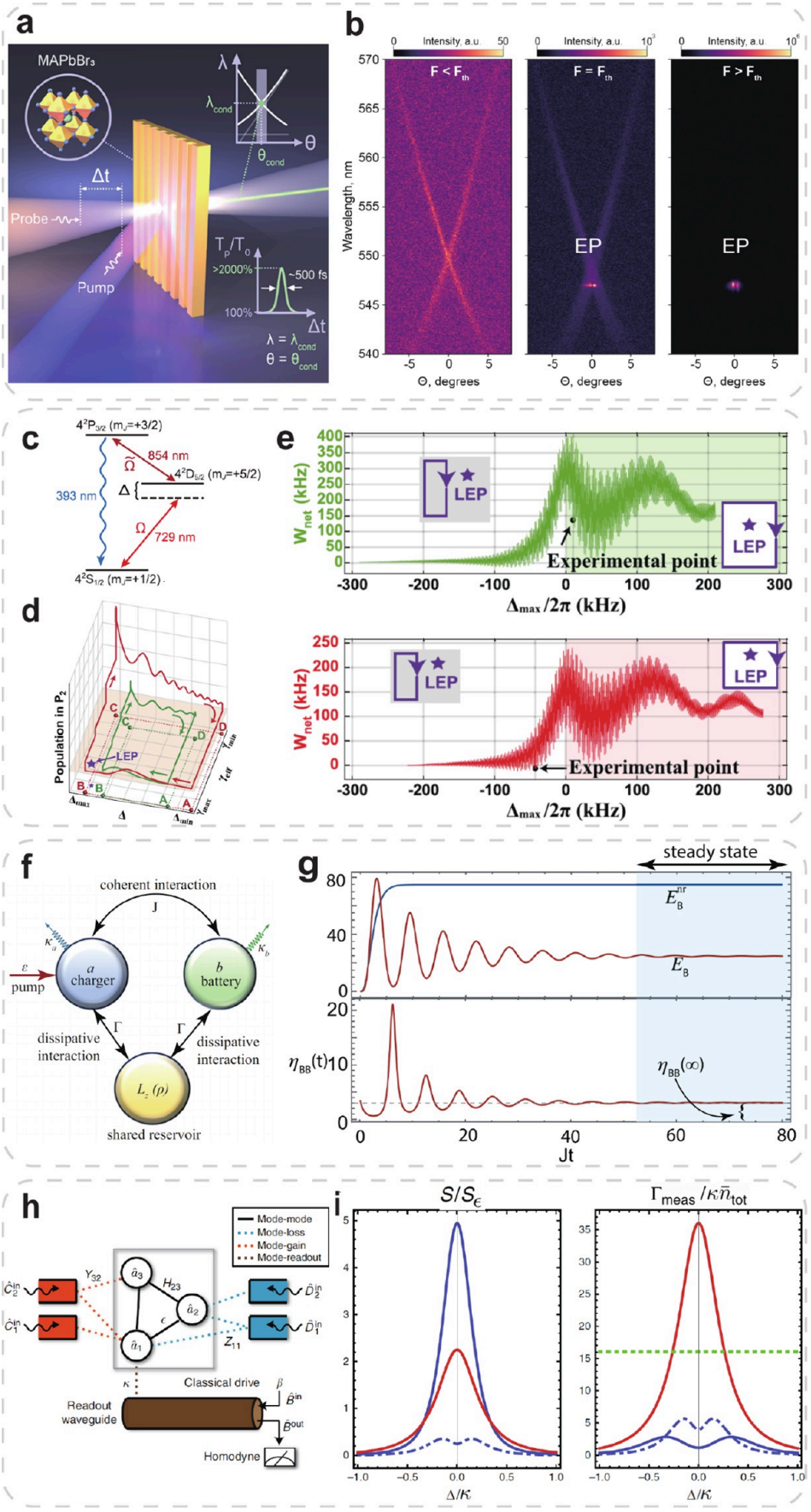

Figure 8. Functional devices based on quantum EPs. (a) Conceptual drawing of the experiment and the studied phenomenon of ultrafast optical modulation in the perovskite metasurface. (b) Angle-resolved emission spectra of perovskite metasurface for the pump fluence

https://doi.org/10.1021/acsnano.4c15648
ACS Nano XXXX, XXX, XXX−XXX

Figure 8. continued

below, equal, and above the lasing threshold.[183] Adapted from ref 183. Copyright 2024 American Chemical Society. (c) Level scheme of $^{40}Ca^{+}$ ion driven by lasers. (d) Simulations of the populations in state $|2\rangle$ with respect to the detuning and the effective decay rate, where the red (green) solid curve represents the evolution of the population with (without) the LEP encircled. (e) Numerical simulation showing the dependence of the net work of the big (top) and small (bottom) quantum heat engines cycles.[50] Adapted with permission from ref 50. Copyright 2023 American Physical Society. (f) Schematic representation of the nonreciprocal quantum battery system. (g) The energy of the battery in reciprocal E_B and nonreciprocal E_B^{nr} regimes (top) and the corresponding enhancement $\eta_{BB} = E_B^{nr}/E_B$ (bottom).[49] Adapted with permission from ref 49. Copyright 2024 American Physical Society. (h) General dispersive measurement setup consists of resonant modes (circles) that interact via a parameter dependent non-Hermitian Hamiltonian. Standard analyses consider only the non-Hermitian dynamics of mode amplitude (region inside the gray rectangle), while an open quantum system requires the inclusion of coupling to gain/loss baths and a readout waveguide. (i) Signal power and measurement rate. Blue dot-dashed: Reciprocal system with an exceptional point but no gain. Blue solid: Reciprocal system with exceptional point and gain. Red: nonreciprocal system. Green dotted: Bound of fundamental reciprocal system.[184] Adapted with permission from ref 184. Copyright 2018 The Authors. Published by Springer Nature, licensed under CC-BY 4.0.

non-Hermitian Hamiltonian description. In the stationary regime, the manipulation of quantum states accessing the EPs has been achieved in both atomic[54,177,178] and diverse coupled quantum systems.[31,60]

The altered coherent and dissipative features of quantum states at the EPs give rise to plentiful quantum applications. In the coupled quantum systems, for example, the critical coupling strength for light-matter interaction entering the strong-coupling regime corresponds to an EP2 for a coupled two component system and thus can be significantly reduced through line width matching at the EP2. This method has been applied in a recent study of a strong plasmon-exciton coupling system, as shown in Figure 7a and b, which has resulted in the significantly improved success rate of achieving the single-exciton strong coupling with plasmon from about 1% to about 80%.[42] It is worth emphasizing that the EPs and PT symmetry implemented in many studies of non-Hermitian quantum systems do not render the quantum features of eigenstates, such as photon statistics, quantum interference, and quantum entanglement. The first measurement of actual quantum features has been achieved in a passive PT-symmetric system consisting of two evanescently coupled optical waveguides,[30,179] as shown in Figure 7c. One of them is lossy, while another is lossless. The PT symmetry exhibits in the Liouvillian space, and thus the system supports an LEP. Individual photons are launched into the waveguides and couple between them. The outputs of the waveguides are measured by photon detectors. The results of two-photon Hong−Ou−Mandel (HOM) interference show that the location of the HOM dip corresponding to destructive interference in this non-Hermitian setup is not consistent with that of the Hermitian one, but shifts to a shorter distance, as shown in Figure 7d. The work demonstrated the quantitatively different quantum nature with non-Hermiticity, and more importantly, it reveals a quantum conundrum that just the possibility of losing a photon can alter the quantum dynamics, even though this photon has finally survived. In another theoretical study, the quantum interference is anticipated to hide the phase transition in a passive PT-symmetric quantum optical system at the few-photon level.[31]

An important application scenario of steering the quantum state by the EP is to generate entanglement between two quantum states, which is a key resource for quantum information technologies ranging from quantum sensing to quantum computing. In a cavity magnon system, PT symmetry can be spontaneously broken in the energy level attraction of magnons and cavity photons. At two EP2s and the PT-broken phase, the magnon and photon form a high-fidelity Bell state with maximum entanglement;[180] see Figure 7e and f. Notably, this entanglement is steady and robust against environmental perturbations, contradicting the general expectation of stability when the PT symmetry is broken. As a comparison, the steady entanglement is replaced by an oscillating one. In a work of studying the entanglement between two coupled qubits, it has been shown that, as the coupled system operated in proximity to an EP4, the entanglement generates at a significantly shorter time scale due to the degeneracies of the eigenstates at the EP4 and allows weaker coupling strength for achieving the maximally entangled state,[28] as shown in Figure 7g−i. Interestingly, the increasingly sharp change in the differential phase of two states on approaching the EP4 suggests that the entanglement generation near the EP4 can provide a sensitive measure of the magnitude of the qubit coupling. In another work of entanglement generation between two qubits with Ising-type interaction, the speed up of entanglement generation has also been observed by comparing with the Hermitian counterpart.[181] In addition, EPs are found to induce exceptional entanglement phenomena, such as collapse-revival and steady-state entanglement. For a many-spin system consisting of non-Hermitian XY spins, it has been shown that high-fidelity W, distant Bell, and GHZ states can be generated in the dynamical process near EPs.[182] While in an experimental setup of all-optical quantum walk supporting the exceptional lines, the generation of the entangled states has been found to be insensitive to the incident state, in stark contrast to the case without exceptional lines.[175] This scheme thus provides a useful method to generate robust entangled states by harnessing the advantage of exceptional lines that are less susceptible to quantum decoherence. Apart from the pure matter (qubit) or light (photon) systems, the entangled light-matter states, i.e., the so-called dressed states, can be generated through strong light-matter interaction. Based on a circuit QED setup of coupled superconducting qubit and decaying resonator, the emergence of maximally entangled states can be observed by encircling the EP2,[78] as shown in Figure 7j−m. These states exhibit an entanglement transition at EP2, characterized by a discontinuity in the derivative of concurrence with respect to the control parameter. This transition signifies a radical departure from classical physics and underscores the nonclassical nature of non-Hermitian quantum mechanics.

3.6. Small-Scale Functional Quantum Devices Based on EPs. The demonstration of exotic features of quantum EPs has triggered the development of functional quantum devices. For example, an ultrafast optical modulation enabled by an EP2 has been demonstrated based on exciton−polariton

https://doi.org/10.1021/acsnano.4c15648
ACS Nano XXXX, XXX, XXX−XXX

condensation.[183] The device has been designed using an MAPbBr3 perovskite metasurface, as shown in Figure 8a−b, where an EP2 is introduced to enhance the accumulation of boson exciton−polaritons in the condensed states. The modulation demonstrates a remarkable 2500% optical signal modulation accomplished with an exceptionally short modulation time of 440 fs. This level of modulation depth is unprecedented in the visible range for modulators because of the degeneracies at the EPs.

On the other hand, the properties of chiral state transfer at the EPs can be applied to enhance the performance of quantum devices. Taking a quantum heat engine as an example, it extracts work from thermal baths and features as a non-Hermitian quantum system.[185] Based on a single trapped $^{40}Ca^{+}$ ion in a linear Paul trap, Zhang et al. constructed an effective qubit with a controllable drive and decay to build a quantum Otto engine, whose temperature is linked to the populations of two energy levels. The variation in populations can thus reflect the heat exchange due to the coupling to the hot and cold baths, which correspond to the strong and weak drives, respectively. By tuning the ratio of drive to decay, the heat engine can be operated to work at an LEP.[186] As shown in Figure 8c−e, they revealed that running the engine during the isochoric heating and cooling strokes of an Otto cycle in the PT-exact and PT-broken phases, respectively, results in higher work output, power, and efficiency compared with executing the entire cycle in the PT-exact phase. The finding is significant as it suggests that the control of a quantum heat engine can be optimized by leveraging the properties of LEPs, in contrast to the conventional view that the coherence in the isochoric strokes is crucial for enhancing the performance. In subsequent works of the same group, the engine cycle of a quantum heat engine has been designed to dynamically encircle an LEP. They observed that the quantum heat engine produces a positive net work when the cycle includes the encircling of an LEP.[50] This is attributed to the Landau−Zener−Stückelberg process, which is influenced by the eigenenergy landscape near the LEP and its topological phase transition under decoherence. These two representative works established a link between the performance of a quantum heat engine and the topological effects originating from encircling an LEP, demonstrating the great ability of an LEP in controlling the quantum heat engines and thermodynamic processes. On the other hand, chiral quantum heating and cooling have been achieved by encircling of an LEP due to the breakdown of adiabaticity.[187] Despite the advantages of encircling an EP, recent studies have pointed out that a quantum Otto cycle at an EP3 is steady, while it exhibits divergent behavior at an EP2,[188] and the work fluctuations of a nonequilibrium system are still constrained by the Jarzynski equality even if its Hamiltonian is non-Hermitian and features an LEP.[63] These findings open new possibilities for LEP-enabled control of quantum heat engines and quantum thermodynamic processes in open quantum systems. While in the nanophotonic platform, Choi et al. proposed a nonlinear integrated optical device involving a coupled-waveguide structure that supports parametric evolution influenced by gain saturation nonlinearity.[189] The architecture can support an EP2 and exhibits highly nonreciprocal behavior over a broad spectrum by encircling the EP. Especially, strictly nonreciprocal optical transmission with a forward-to-backward transmission ratio exceeding 10 dB and high forward transmission efficiency (approximately 100%) over a bandwidth approaching 100 THz has been demonstrated through rigorous numerical simulations. This superior performance is attributed to the non-Hermitian features of the system, allowing for the breaking of reciprocity in transmission, which is not possible to achieve in a linear and stationary Hermitian system without the EP.

Besides the properties of degeneracy, the higher dimension of the EPs also holds great potential in applications. In this regard, the chiral EPs featuring a two-dimensional surface in the parameter space can offer unique advantages since its occurrence is in general accompanied by nonreciprocal interactions. Taking the quantum battery as an example (see Figure 8f−g), by introducing the chiral EPs between the charger and battery through the reservoir engineering, the energy transfer of the charging process is more efficient and results in a 4-fold increase in battery energy compared to the conventional charger-battery systems, even in the presence of local dissipation.[49] The substantial increase in energy storage is attributed to effectively suppressing the energy backflow from the battery to the charger by the introduced chiral EPs. In the quantum battery constructed by a chain of spins, the emerging EPs have been also found to produce an increased power output compared to traditional Hermitian chargers, and the improvement persists even as the system size increases.[48] Another important application of the chiral EPs is to break down the fundamental sensitivity limit of a quantum sensor based on reciprocal interactions. As discussed in the previous subsection, a quantum sensor operated at the EPs in principle offers no SNR enhancement due to the existence of quantum noise. However, with the nonreciprocal interaction accompanied by the chiral EPs, as shown in Figure 8h−i, the fundamental bounds on the signal power and SNR of quantum sensors can exceed the reciprocal counterparts.[184] Such a nonreciprocal quantum sensor can be realized based on a linear coupled-mode quantum system with aforementioned reservoir engineering for a quantum battery. The signal can be detected by a realistic measurement protocol of coherent driving and homodyne detection. Besides the reservoir engineering, the chiral EPs have also been found to be implemented by circularly polarized QEs.[190] Therefore, the chiral EPs are anticipated to advance a variety of functional quantum devices, such as logical gates,[191] quantum routers,[192] quantum sensors,[193] etc.

4. CONCLUSION AND FUTURE OUTLOOK

Originating from quantum mechanics, the striking concept of the EPs is related to the PT symmetry and associated eigenenergy spectra of the non-Hermitian Hamiltonians. The flexibility of the classical photonic structures allows for implementing PT symmetry and creating the EPs with ease of using optical gain and loss. This leads to the exploration of the non-Hermitian physics in photonics but admits a different interpretation of the PT symmetry from the original idea. The PT symmetry in photonics manifests as a balance of energy growth and decay that gives rise to stable steady states at the EPs. Many effects and applications of the EPs are attributed to the coalesced eigenstates at the degeneracies of parameter space, a feature in stark contrast to the Hermitian degeneracies with the preserved orthogonality of eigenstates. After the vicennial flourishing in classical photonics, research interest recently has trended to refocus on the effect of the EPs in quantum systems.

While the concepts and properties of the EPs can be translated from the classical systems, there is still huge room

https://doi.org/10.1021/acsnano.4c15648
ACS Nano XXXX, XXX, XXX−XXX

and exciting opportunities for exploring the new physics and advanced applications of the quantum EPs. The peculiar features of the quantum EPs, originating from the very skewed state space and associated topology, enable plentiful possibilities for a wide range of applications, as we discussed in this review. Different from those that arise in the typical scenario of classical photonics, where the coupled two or multiple modes with different gain and loss are involved, the applications for the non-Hermitian quantum systems require consideration of the effects of dephasing, quantum jump, and quantum noise, which cannot be encapsulated by the approach for the non-Hermitian classical systems. Over the past decade, a great deal of effort has been devoted to exploring the features and applications of quantum EPs, providing an entirely new perspective of dissipation in quantum systems. Though considered as a detrimental effect for Hermitian quantum systems, the dissipation can play a positive role in engineering the non-Hermitian features of an open quantum system and develop quantum devices with functionalities not achievable in Hermitian settings. The additional quantum fluctuations, noises, and amplifying may give rise to unexpected features and counterintuitive phenomena related to the quantum EPs, and these new elements are expected to be included in the theoretical framework of non-Hermitian quantum physics with more creative endeavors. In this emerging field of quantum EPs, a large portion of works is still theoretical, and the experimental verification and demonstrations are of great importance and highly desirable.

The future direction of the quantum EPs may hide in the implications of the term "quantum", which has multiple physical meanings in different quantum systems and can be interpreted at least in three aspects. The simplest implication of quantum EPs is the EPs hosting in a quantum system, which has been extensively studied in theory and experimentally demonstrated in diverse quantum platforms, as discussed above. Nevertheless, this interpretation cannot offer more physical insights unless we inquire about the different features of the EPs in quantum systems from those in classical systems. It derives the second implication of quantum EPs, which means that the EPs originate from quantum effects, such as quantum jump and dephasing, for the LEPs. Typical examples are driven by dissipative superconducting qubits and quantum heat engines. Further research can explore the quantum EPs connecting with topological physics[194−198] and nonequilibrium systems,[199−201] and other kinds of symmetry like anti-PT symmetry[202−205] and supersymmetry,[206] which may find important applications in the cutting-edge technologies, including but not limited to the non-Hermitian sensing,[207,208] time crystals,[209−211] and frequency combs.[212] While the latter has been mostly studied classically, it is fundamentally governed by the dynamics of quantized parametric processes. This indicates another implication of the quantum EPs from the perspective of applications. In this perspective, the quantum EPs refer to the EPs that produce the quantum effects or alter the quantum nature of the system or the state, such as quantum correlations and photon statistics, thus encompassing a wider range of systems including the previous two cases as well as those where the EPs are essentially classical. A representative example discussed in this review is the CEP cavity. While the EPs are obviously classical, the CEP cavity is expected to advance various quantum-optical applications, such as multiphotonic processes,[213−215] nonlinear interactions,[167,216,217] single-photon nonlinearity,[218] strong exciton-photon interactions at room temperature,[219−221] and single-molecule optomechanics by integrating with a plasmonic cavity.[222] Therefore, in the context of future experimental study, the quantum EPs can be observed by detecting the change of quantum nature through quantum state tomography, two-photon HOM, etc., and monitoring the dynamic behavior of quantum states, which are the most direct ways to unveil the effects of the quantum EPs. Of specific importance is the ability to achieve *in situ* control of system parameters, which is scarce but nonetheless crucial for developing advanced EP-based technologies like quantum heat engines[223] and EP-enhanced real-time Raman spectroscopy.[193,224] In this regard, the higher-dimensional and higher-order quantum EPs can offer more degrees of freedom to access and feature high robustness against experimental errors, which would be beneficial to achieve precise dynamic control, and they still face challenges for open quantum systems. Finally, the theoretical predictions related to the applications of quantum EPs like quantum sensing will certainly encourage further experimental verification and development of practical quantum devices.

AUTHOR INFORMATION

Corresponding Author

Xue-Hua Wang − *State Key Laboratory of Optoelectronic Materials and Technologies, School of Physics, Sun Yat-sen University, Guangzhou 510275, China;* orcid.org/0000-0003-1324-1471; Email: wangxueh@mail.sysu.edu.cn

Authors

Yu-Wei Lu − *Quantum Science Center of Guangdong-Hong Kong-Macao Greater Bay Area (Guangdong), Shenzhen 518045, China;* orcid.org/0000-0002-3174-6812

Wei Li − *State Key Laboratory of Optoelectronic Materials and Technologies, School of Physics, Sun Yat-sen University, Guangzhou 510275, China*

Complete contact information is available at: https://pubs.acs.org/10.1021/acsnano.4c15648

Author Contributions

The manuscript was written through contributions of all authors. All authors have given approval to the final version of the manuscript.

Notes

The authors declare no competing financial interest.

ACKNOWLEDGMENTS

This project was supported by the National Key R&D Program of China (No. 2021YFA1400800), the National Natural Science Foundation of China (Nos. 12334017, 62205061, 12274192), and the Guangdong Provincial Quantum Science Strategic Initiative (GDZX2306002; GDZX2406001).

ABBREVIATIONS

PT, parity-time; EPs, exceptional points; LEPs, Liouvillian exceptional points; HEPs, Hamiltonian exceptional points; EP*k*s, exceptional points with *k*-fold degeneracy of the eigenenergies and eigenstates; WGM, whispering gallery mode; CEP, chiral exceptional points; QED, cavity quantum electrodynamics; QD, quantum dot; NV, nitrogen-vacancy; QFI, quantum Fisher information; SNR, signal-to-noise ratio; QE, quantum emitter; SE, spontaneous emission; LDOS, local density of states; CCW, counterclockwise; CW, clockwise;

https://doi.org/10.1021/acsnano.4c15648
ACS Nano XXXX, XXX, XXX−XXX

QNM, quasi-normal mode; 1PB, single-photon blockade; PIM, pump-induced magnon mode; KM, Kittel mode; HOM, Hong−Ou−Mandel

Vocabulary

Nonclassical light: The light field that cannot be described by classical electromagnetic theory and requires the principles of quantum mechanics to fully understand its behavior. Here the nonclassical light is specially referred to as the antibunching light in single-photon Fock states.

Strong light-matter interaction: A regime that the coherent coupling between the photons and emitters involved in the interaction can surpass the dissipation of the whole system. It leads to the reversible energy exchange between two components. A typical example is the Rabi oscillation in cavity quantum electrodynamics.

Purcell effect: A phenomenon in quantum electrodynamics where the spontaneous emission rate of a quantum emitter system, such as an atom or a quantum dot, can be enhanced or suppressed by the surrounding environment as a consequence of the enhancement or decrease of the local density of photonic states at the emitter's position, respectively.

Signal-to-noise ratio: A measure used in science and engineering to quantify the level of a desired signal to the level of background noise. It is often defined as the ratio of the power of the signal to the power of the noise that is disturbing the desired signal. A higher signal-to-noise ratio indicates a greater level of the desired signal compared to the background noise.

Quantum heat engine: The quantum systems that utilize quantum mechanics to perform thermodynamic work cycles and exhibit unique properties that are not found in their classical counterparts.

Frequency combs: The specialized lasers that were originally developed to support the world's most precise atomic clocks, enabling the precise transfer of phase and frequency information from a high-stability reference to hundreds of thousands of tones in the optical domain. The frequency combs can act like a ruler for light, allowing for the precise measurement of light frequencies across various parts of the electromagnetic spectrum, from infrared and ultraviolet to visible light.

REFERENCES

(1) Özdemir, S. K.; Rotter, S.; Nori, F.; Yang, L. Parity-time symmetry and exceptional points in photonics. *Nat. Mater.* **2019**, *18* (8), 783−798.

(2) Feng, L.; El-Ganainy, R.; Ge, L. Non-Hermitian photonics based on parity-time symmetry. *Nat. Photonics* **2017**, *11* (12), 752−762.

(3) Miri, M.-A.; Alù, A. Exceptional points in optics and photonics. *Science* **2019**, *363* (6422), No. eaar7709.

(4) El-Ganainy, R.; Makris, K. G.; Khajavikhan, M.; Musslimani, Z. H.; Rotter, S.; Christodoulides, D. N. Non-Hermitian physics and PT symmetry. *Nat. Phys.* **2018**, *14* (1), 11−19.

(5) Tang, W.; Jiang, X.; Ding, K.; Xiao, Y.-X.; Zhang, Z.-Q.; Chan, C. T.; Ma, G. Exceptional nexus with a hybrid topological invariant. *Science* **2020**, *370* (6520), 1077−1080.

(6) Assawaworrarit, S.; Yu, X.; Fan, S. Robust wireless power transfer using a nonlinear parity-time-symmetric circuit. *Nature* **2017**, *546* (7658), 387−390.

(7) Zhao, W.; Zhang, Y.; Gao, Z.; Peng, D.; Kou, J.-l.; Lu, Y.-q.; El-Ganainy, R.; Özdemir, S. K.; Zhong, Q. Exceptional points induced by unidirectional coupling in electronic circuits. *Nat. Commun.* **2024**, *15* (1), 9907.

(8) Xu, H.; Mason, D.; Jiang, L.; Harris, J. G. E. Topological energy transfer in an optomechanical system with exceptional points. *Nature* **2016**, *537* (7618), 80−83.

(9) Wu, N.; Cui, K.; Xu, Q.; Feng, X.; Liu, F.; Zhang, W.; Huang, Y. On-chip mechanical exceptional points based on an optomechanical zipper cavity. *Science Advances* **2023**, *9* (3), No. eabp8892.

(10) Li, Y.; Peng, Y.-G.; Han, L.; Miri, M.-A.; Li, W.; Xiao, M.; Zhu, X.-F.; Zhao, J.; Alù, A.; Fan, S.; Qiu, C.-W. Anti-parity-time symmetry in diffusive systems. *Science* **2019**, *364* (6436), 170−173.

(11) Gamow, G. Zur Quantentheorie des Atomkernes. *Zeitschrift für Physik* **1928**, *51* (3), 204−212.

(12) Siegert, A. J. F. On the Derivation of the Dispersion Formula for Nuclear Reactions. *Phys. Rev.* **1939**, *56* (8), 750−752.

(13) Feshbach, H.; Porter, C. E.; Weisskopf, V. F. Model for Nuclear Reactions with Neutrons. *Phys. Rev.* **1954**, *96* (2), 448−464.

(14) Bender, C. M.; Boettcher, S. Real Spectra in Non-Hermitian Hamiltonians Having PT Symmetry. *Phys. Rev. Lett.* **1998**, *80* (24), 5243−5246.

(15) Larson, J.; Qvarfort, S. Exceptional Points and Exponential Sensitivity for Periodically Driven Lindblad Equations. *Open Systems & Information Dynamics* **2023**, *30* (02), 2350008.

(16) Ashida, Y.; Gong, Z.; Ueda, M. Non-Hermitian physics. *Adv. Phys.* **2020**, *69* (3), 249−435.

(17) Parto, M.; Liu, Y. G. N.; Bahari, B.; Khajavikhan, M.; Christodoulides, D. N. Non-Hermitian and topological photonics: optics at an exceptional point. *Nanophotonics* **2020**, *10* (1), 403−423.

(18) Ding, K.; Fang, C.; Ma, G. Non-Hermitian topology and exceptional-point geometries. *Nature Reviews Physics* **2022**, *4* (12), 745−760.

(19) Bergholtz, E. J.; Budich, J. C.; Kunst, F. K. Exceptional topology of non-Hermitian systems. *Rev. Mod. Phys.* **2021**, *93* (1), 015005.

(20) Luitz, D. J.; Piazza, F. Exceptional points and the topology of quantum many-body spectra. *Physical Review Research* **2019**, *1* (3), 033051.

(21) Heiss, W. D. The physics of exceptional points. *Journal of Physics A: Mathematical and Theoretical* **2012**, *45* (44), 444016.

(22) Müller, M.; Rotter, I. Exceptional points in open quantum systems. *Journal of Physics A: Mathematical and Theoretical* **2008**, *41* (24), 244018.

(23) Roccati, F.; Palma, G. M.; Ciccarello, F.; Bagarello, F. Non-Hermitian Physics and Master Equations. *Open Systems & Information Dynamics* **2022**, *29* (01), 2250004.

(24) Minganti, F.; Miranowicz, A.; Chhajlany, R. W.; Nori, F. Quantum exceptional points of non-Hermitian Hamiltonians and Liouvillians: The effects of quantum jumps. *Phys. Rev. A* **2019**, *100* (6), 062131.

(25) Ren, Z.; Liu, D.; Zhao, E.; He, C.; Pak, K. K.; Li, J.; Jo, G.-B. Chiral control of quantum states in non-Hermitian spin-orbit-coupled fermions. *Nat. Phys.* **2022**, *18* (4), 385−389.

(26) Gao, T.; Li, G.; Estrecho, E.; Liew, T. C. H.; Comber-Todd, D.; Nalitov, A.; Steger, M.; West, K.; Pfeiffer, L.; Snoke, D. W.; Kavokin, A. V.; Truscott, A. G.; Ostrovskaya, E. A. Chiral Modes at Exceptional Points in Exciton-Polariton Quantum Fluids. *Phys. Rev. Lett.* **2018**, *120* (6), 065301.

(27) Lee, C. H. Exceptional Bound States and Negative Entanglement Entropy. *Phys. Rev. Lett.* **2022**, *128* (1), 010402.

(28) Li, Z.-Z.; Chen, W.; Abbasi, M.; Murch, K. W.; Whaley, K. B. Speeding Up Entanglement Generation by Proximity to Higher-Order Exceptional Points. *Phys. Rev. Lett.* **2023**, *131* (10), 100202.

(29) Fang, Y.-L.; Zhao, J.-L.; Chen, D.-X.; Zhou, Y.-H.; Zhang, Y.; Wu, Q.-C.; Yang, C.-P.; Nori, F. Entanglement dynamics in anti-PT-symmetric systems. *Physical Review Research* **2022**, *4* (3), 033022.

(30) Klauck, F.; Teuber, L.; Ornigotti, M.; Heinrich, M.; Scheel, S.; Szameit, A. Observation of PT-symmetric quantum interference. *Nat. Photonics* **2019**, *13* (12), 883−887.

(31) Longhi, S. Quantum interference and exceptional points. *Opt. Lett.* **2018**, *43* (21), 5371−5374.

(32) Chen, W.; Abbasi, M.; Ha, B.; Erdamar, S.; Joglekar, Y. N.; Murch, K. W. Decoherence-Induced Exceptional Points in a

https://doi.org/10.1021/acsnano.4c15648
ACS Nano XXXX, XXX, XXX−XXX

Dissipative Superconducting Qubit. *Phys. Rev. Lett.* **2022**, *128* (11), 110402.
(33) Huang, R.; Özdemir, S. K.; Liao, J.-Q.; Minganti, F.; Kuang, L.-M.; Nori, F.; Jing, H. Exceptional Photon Blockade: Engineering Photon Blockade with Chiral Exceptional Points. *Laser & Photonics Reviews* **2022**, *16* (7), 2100430.
(34) Chen, H.-Z.; Liu, T.; Luan, H.-Y.; Liu, R.-J.; Wang, X.-Y.; Zhu, X.-F.; Li, Y.-B.; Gu, Z.-M.; Liang, S.-J.; Gao, H.; Lu, L.; Ge, L.; Zhang, S.; Zhu, J.; Ma, R.-M. Revealing the missing dimension at an exceptional point. *Nat. Phys.* **2020**, *16*, 571−578.
(35) Zhong, Q.; Hashemi, A.; Özdemir, S. K.; El-Ganainy, R. Control of spontaneous emission dynamics in microcavities with chiral exceptional surfaces. *Physical Review Research* **2021**, *3* (1), 013220.
(36) Agarwal, G. S. Control of the Purcell effect via unexcited atoms and exceptional points. *Physical Review Research* **2024**, *6* (1), L012050.
(37) Lin, Z.; Pick, A.; Lončar, M.; Rodriguez, A. W. Enhanced Spontaneous Emission at Third-Order Dirac Exceptional Points in Inverse-Designed Photonic Crystals. *Phys. Rev. Lett.* **2016**, *117* (10), 107402.
(38) Ferrier, L.; Bouteyre, P.; Pick, A.; Cueff, S.; Dang, N. H. M.; Diederichs, C.; Belarouci, A.; Benyattou, T.; Zhao, J. X.; Su, R.; Xing, J.; Xiong, Q.; Nguyen, H. S. Unveiling the Enhancement of Spontaneous Emission at Exceptional Points. *Phys. Rev. Lett.* **2022**, *129* (8), 083602.
(39) Zhang, X.; Liu, Q.; Zhang, Q.; Li, Z.; Ma, Y.; Gong, Q.; Gu, Y. Loss-induced Purcell enhancement in PT-broken whispering gallery microcavities. *Opt. Lett.* **2023**, *48* (15), 4069−4072.
(40) Lu, Y.-W.; Liu, J.-F.; Liu, R.; Jiang, H.-X. Enhanced quantum coherence of plasmonic resonances with a chiral exceptional points. *Communications Physics* **2024**, *7* (1), 166.
(41) Khanbekyan, M.; Wiersig, J. Decay suppression of spontaneous emission of a single emitter in a high-Q cavity at exceptional points. *Physical Review Research* **2020**, *2* (2), 023375.
(42) Li, W.; Liu, R.; Li, J.; Zhong, J.; Lu, Y.-W.; Chen, H.; Wang, X.-H. Highly Efficient Single-Exciton Strong Coupling with Plasmons by Lowering Critical Interaction Strength at an Exceptional Point. *Phys. Rev. Lett.* **2023**, *130* (14), 143601.
(43) Ernzerhof, M.; Giguère, A.; Mayou, D. Non-Hermitian quantum mechanics and exceptional points in molecular electronics. *J. Chem. Phys.* **2020**, *152* (24), 244119.
(44) Hou, S.; Wu, T.; Zhang, W.; Zhang, X. Strongly Enhanced Raman Optical Activity of Chiral Molecules by Vector Exceptional Points. *J. Phys. Chem. C* **2020**, *124* (45), 24970−24977.
(45) Marie, A.; Burton, H. G. A.; Loos, P.-F. Perturbation theory in the complex plane: exceptional points and where to find them. *J. Phys.: Condens. Matter* **2021**, *33* (28), 283001.
(46) Barman, H.; Valliapan, S. A tale of two kinds of exceptional point in a hydrogen molecule. *J. Phys.: Condens. Matter* **2022**, *34* (20), 205601.
(47) Wang, C.; Rao, J.; Chen, Z.; Zhao, K.; Sun, L.; Yao, B.; Yu, T.; Wang, Y.-P.; Lu, W. Enhancement of magnonic frequency combs by exceptional points. *Nat. Phys.* **2024**, *20*, 1139.
(48) Konar, T. K.; Lakkaraju, L. G. C.; Sen, A. Quantum battery with non-Hermitian charging. *Phys. Rev. A* **2024**, *109* (4), 042207.
(49) Ahmadi, B.; Mazurek, P.; Horodecki, P.; Barzanjeh, S. Nonreciprocal Quantum Batteries. *Phys. Rev. Lett.* **2024**, *132* (21), 210402.
(50) Bu, J. T.; Zhang, J. Q.; Ding, G. Y.; Li, J. C.; Zhang, J. W.; Wang, B.; Ding, W. Q.; Yuan, W. F.; Chen, L.; Özdemir, S. K.; Zhou, F.; Jing, H.; Feng, M. Enhancement of Quantum Heat Engine by Encircling a Liouvillian Exceptional Point. *Phys. Rev. Lett.* **2023**, *130* (11), 110402.
(51) Zhang, M.; Sweeney, W.; Hsu, C. W.; Yang, L.; Stone, A. D.; Jiang, L. Quantum Noise Theory of Exceptional Point Amplifying Sensors. *Phys. Rev. Lett.* **2019**, *123* (18), 180501.
(52) Wiersig, J. Robustness of exceptional-point-based sensors against parametric noise: The role of Hamiltonian and Liouvillian degeneracies. *Phys. Rev. A* **2020**, *101* (5), 053846.
(53) Schäfer, R.; Budich, J. C.; Luitz, D. J. Symmetry protected exceptional points of interacting fermions. *Physical Review Research* **2022**, *4* (3), 033181.
(54) Wu, Y.; Liu, W.; Geng, J.; Song, X.; Ye, X.; Duan, C. K.; Rong, X.; Du, J. Observation of parity-time symmetry breaking in a single-spin system. *Science* **2019**, *364* (6443), 878−880.
(55) Naghiloo, M.; Abbasi, M.; Joglekar, Y. N.; Murch, K. W. Quantum state tomography across the exceptional point in a single dissipative qubit. *Nat. Phys.* **2019**, *15* (12), 1232−1236.
(56) Wang, C.; Li, N.; Xie, J.; Ding, C.; Ji, Z.; Xiao, L.; Jia, S.; Yan, B.; Hu, Y.; Zhao, Y. Exceptional Nexus in Bose−Einstein Condensates with Collective Dissipation. *Phys. Rev. Lett.* **2024**, *132* (25), 253401.
(57) Liang, C.; Tang, Y.; Xu, A.-N.; Liu, Y.-C. Observation of Exceptional Points in Thermal Atomic Ensembles. *Phys. Rev. Lett.* **2023**, *130* (26), 263601.
(58) Wang, C.; Fu, Z.; Mao, W.; Qie, J.; Stone, A. D.; Yang, L. Non-Hermitian optics and photonics: from classical to quantum. *Advances in Optics and Photonics* **2023**, *15* (2), 442−523.
(59) Jing, H.; Özdemir, S. K.; Lü, H.; Nori, F. High-order exceptional points in optomechanics. *Sci. Rep.* **2017**, *7* (1), 3386.
(60) Zhang, D.; Luo, X.-Q.; Wang, Y.-P.; Li, T.-F.; You, J. Q. Observation of the exceptional point in cavity magnon-polaritons. *Nat. Commun.* **2017**, *8* (1), 1368.
(61) Zhang, X.; Ding, K.; Zhou, X.; Xu, J.; Jin, D. Experimental Observation of an Exceptional Surface in Synthetic Dimensions with Magnon Polaritons. *Phys. Rev. Lett.* **2019**, *123* (23), 237202.
(62) Chen, W.; Abbasi, M.; Joglekar, Y. N.; Murch, K. W. Quantum Jumps in the Non-Hermitian Dynamics of a Superconducting Qubit. *Phys. Rev. Lett.* **2021**, *127* (14), 140504.
(63) Erdamar, S.; Abbasi, M.; Ha, B.; Chen, W.; Muldoon, J.; Joglekar, Y.; Murch, K. W. Constraining work fluctuations of non-Hermitian dynamics across the exceptional point of a superconducting qubit. *Physical Review Research* **2024**, *6* (2), L022013.
(64) Wu, Y.; Wang, Y.; Ye, X.; Liu, W.; Niu, Z.; Duan, C.-K.; Wang, Y.; Rong, X.; Du, J. Third-order exceptional line in a nitrogen-vacancy spin system. *Nat. Nanotechnol.* **2024**, *19* (2), 160−165.
(65) He, P.; Fu, J.-H.; Zhang, D.-W.; Zhu, S.-L. Double exceptional links in a three-dimensional dissipative cold atomic gas. *Phys. Rev. A* **2020**, *102* (2), 023308.
(66) Zhong, Q.; Ren, J.; Khajavikhan, M.; Christodoulides, D. N.; Ozdemir, S. K.; El-Ganainy, R. Sensing with Exceptional Surfaces in Order to Combine Sensitivity with Robustness. *Phys. Rev. Lett.* **2019**, *122* (15), 153902.
(67) Li, J.; Li, W.; Feng, Y.; Wang, J.; Yao, Y.; Sun, Y.; Zou, Y.; Wang, J.; He, F.; Duan, J.; Chen, G. J.; Shum, P. P.; Xu, X. On-Chip Fabrication-Tolerant Exceptional Points Based on Dual-Scatterer Engineering. *Nano Lett.* **2024**, *24* (13), 3906−3913.
(68) Lu, Y.-W.; Liu, J.-F.; Liu, R.; Su, R.; Wang, X.-H. Quantum exceptional chamber induced by large nondipole effect of a quantum dot coupled to a nano-plasmonic resonator. *Nanophotonics* **2021**, *10* (9), 2431−2440.
(69) Duggan, R.; Mann, S. A.; Alù, A. Limitations of Sensing at an Exceptional Point. *ACS Photonics* **2022**, *9* (5), 1554.
(70) Langbein, W. No exceptional precision of exceptional-point sensors. *Phys. Rev. A* **2018**, *98* (2), 023805.
(71) Ding, W.; Wang, X.; Chen, S. Fundamental Sensitivity Limits for Non-Hermitian Quantum Sensors. *Phys. Rev. Lett.* **2023**, *131* (16), 160801.
(72) Loughlin, H.; Sudhir, V. Exceptional-Point Sensors Offer No Fundamental Signal-to-Noise Ratio Enhancement. *Phys. Rev. Lett.* **2024**, *132* (24), 243601.
(73) Waghela, C.; Dasgupta, S. Simulation of exceptional-point systems on quantum computers for quantum sensing. *AVS Quantum Science* **2024**, *6* (1), 014403.
(74) Wong, W. C.; Li, J. Exceptional-point sensing with a quantum interferometer. *New J. Phys.* **2023**, *25* (3), 033018.

https://doi.org/10.1021/acsnano.4c15648
ACS Nano XXXX, XXX, XXX−XXX

(75) Minganti, F.; Arkhipov, I. I.; Miranowicz, A.; Nori, F. Liouvillian spectral collapse in the Scully-Lamb laser model. *Physical Review Research* **2021**, *3* (4), 043197.
(76) Scheel, S.; Szameit, A. PT-symmetric photonic quantum systems with gain and loss do not exist. *Europhys. Lett.* **2018**, *122* (3), 34001.
(77) Arkhipov, I. I.; Miranowicz, A.; Minganti, F.; Nori, F. Quantum and semiclassical exceptional points of a linear system of coupled cavities with losses and gain within the Scully-Lamb laser theory. *Phys. Rev. A* **2020**, *101* (1), 013812.
(78) Han, P.-R.; Wu, F.; Huang, X.-J.; Wu, H.-Z.; Zou, C.-L.; Yi, W.; Zhang, M.; Li, H.; Xu, K.; Zheng, D.; Fan, H.; Wen, J.; Yang, Z.-B.; Zheng, S.-B. Exceptional Entanglement Phenomena: Non-Hermiticity Meeting Nonclassicality. *Phys. Rev. Lett.* **2023**, *131* (26), 260201.
(79) Bian, Z.; Xiao, L.; Wang, K.; Onanga, F. A.; Ruzicka, F.; Yi, W.; Joglekar, Y. N.; Xue, P. Quantum information dynamics in a high-dimensional parity-time-symmetric system. *Phys. Rev. A* **2020**, *102* (3), 030201.
(80) Tang, J.-S.; Wang, Y.-T.; Yu, S.; He, D.-Y.; Xu, J.-S.; Liu, B.-H.; Chen, G.; Sun, Y.-N.; Sun, K.; Han, Y.-J.; Li, C.-F.; Guo, G.-C. Experimental investigation of the no-signalling principle in parity-time symmetric theory using an open quantum system. *Nat. Photonics* **2016**, *10* (10), 642−646.
(81) Yasir, K. A.; Zhuang, L.; Liu, W.-M. Topological nonlinear optics with spin-orbit coupled Bose−Einstein condensate in cavity. *npj Quantum Information* **2022**, *8* (1), 109.
(82) Youssefi, A.; Kono, S.; Bancora, A.; Chegnizadeh, M.; Pan, J.; Vovk, T.; Kippenberg, T. J. Topological lattices realized in superconducting circuit optomechanics. *Nature* **2022**, *612* (7941), 666−672.
(83) Barrios, G. A.; Albarrán-Arriagada, F.; Cárdenas-López, F. A.; Romero, G.; Retamal, J. C. Role of quantum correlations in light-matter quantum heat engines. *Phys. Rev. A* **2017**, *96* (5), 052119.
(84) Carmichael, H. J. *Statistical Methods in Quantum Optics*; Springer: Berlin, 1999.
(85) Arkhipov, I. I.; Miranowicz, A.; Minganti, F.; Nori, F. Liouvillian exceptional points of any order in dissipative linear bosonic systems: Coherence functions and switching between PT and anti-PT symmetries. *Phys. Rev. A* **2020**, *102* (3), 033715.
(86) Seshadri, N.; Li, A.; Galperin, M. Liouvillian exceptional points of an open driven two-level system. *J. Chem. Phys.* **2024**, *160* (4), 044116.
(87) Brody, D. C. Biorthogonal quantum mechanics. *Journal of Physics A: Mathematical and Theoretical* **2014**, *47* (3), 035305.
(88) Khandelwal, S.; Brunner, N.; Haack, G. Signatures of Liouvillian Exceptional Points in a Quantum Thermal Machine. *PRX Quantum* **2021**, *2* (4), 040346.
(89) Zhou, Y.-L.; Yu, X.-D.; Wu, C.-W.; Li, X.-Q.; Zhang, J.; Li, W.; Chen, P.-X. Accelerating relaxation through Liouvillian exceptional point. *Physical Review Research* **2023**, *5* (4), 043036.
(90) Zhang, J.; Xia, G.; Wu, C.-W.; Chen, T.; Zhang, Q.; Xie, Y.; Su, W.-B.; Wu, W.; Qiu, C.-W.; Chen, P.-X.; Li, W.; Jing, H.; Zhou, Y.-L. Observation of quantum strong Mpemba effect. *Nat. Commun.* **2025**, *16* (1), 301.
(91) Kumar, P.; Snizhko, K.; Gefen, Y.; Rosenow, B. Optimized steering: Quantum state engineering and exceptional points. *Phys. Rev. A* **2022**, *105* (1), L010203.
(92) Gunderson, J.; Muldoon, J.; Murch, K. W.; Joglekar, Y. N. Floquet exceptional contours in Lindblad dynamics with time-periodic drive and dissipation. *Phys. Rev. A* **2021**, *103* (2), 023718.
(93) Lin, J.-D.; Kuo, P.-C.; Lambert, N.; Miranowicz, A.; Nori, F.; Chen, Y.-N. Non-Markovian Quantum Exceptional Points. *Nat. Commun.* **2025**, *16*, 1289.
(94) Perina, J., Jr; Miranowicz, A.; Chimczak, G.; Kowalewska-Kudlaszyk, A. Quantum Liouvillian exceptional and diabolical points for bosonic fields with quadratic Hamiltonians: The Heisenberg-Langevin equation approach. *Quantum* **2022**, *6*, 883.
(95) Peřina, J.; Miranowicz, A.; Kalaga, J. K.; Leoński, W. Unavoidability of nonclassicality loss in PT-symmetric systems. *Phys. Rev. A* **2023**, *108* (3), 033512.
(96) Wakefield, R.; Laing, A.; Joglekar, Y. N. Non-Hermiticity in quantum nonlinear optics through symplectic transformations. *Appl. Phys. Lett.* **2024**, *124* (20), 201103.
(97) Lu, Y.-K.; Peng, P.; Cao, Q.-T.; Xu, D.; Wiersig, J.; Gong, Q.; Xiao, Y.-F. Spontaneous T-symmetry breaking and exceptional points in cavity quantum electrodynamics systems. *Science Bulletin* **2018**, *63* (17), 1096−1100.
(98) Lu, Y.; Tan, H.; Liao, Z. Dressed bound states at chiral exceptional points. *Phys. Rev. A* **2023**, *107* (4), 043714.
(99) Minganti, F.; Miranowicz, A.; Chhajlany, R. W.; Arkhipov, I. I.; Nori, F. Hybrid-Liouvillian formalism connecting exceptional points of non-Hermitian Hamiltonians and Liouvillians via postselection of quantum trajectories. *Phys. Rev. A* **2020**, *101* (6), 062112.
(100) Abo, S.; Tulewicz, P.; Bartkiewicz, K.; Özdemir, S. K.; Miranowicz, A. Experimental Liouvillian exceptional points in a quantum system without Hamiltonian singularities. *New J. Phys.* **2024**, *26* (12), 123032.
(101) Wiersig, J. Review of exceptional point-based sensors. *Photonics Research* **2020**, *8* (9), 1457−1467.
(102) Hodaei, H.; Hassan, A. U.; Wittek, S.; Garcia-Gracia, H.; El-Ganainy, R.; Christodoulides, D. N.; Khajavikhan, M. Enhanced sensitivity at higher-order exceptional points. *Nature* **2017**, *548* (7666), 187−191.
(103) Chen, W.; Kaya Özdemir, S.; Zhao, G.; Wiersig, J.; Yang, L. Exceptional points enhance sensing in an optical microcavity. *Nature* **2017**, *548* (7666), 192−196.
(104) Arkhipov, I. I.; Minganti, F.; Miranowicz, A.; Nori, F. Generating high-order quantum exceptional points in synthetic dimensions. *Phys. Rev. A* **2021**, *104* (1), 012205.
(105) Zhou, X.; Ren, X.; Xiao, D.; Zhang, J.; Huang, R.; Li, Z.; Sun, X.; Wu, X.; Qiu, C.-W.; Nori, F.; Jing, H. Higher-order singularities in phase-tracked electromechanical oscillators. *Nat. Commun.* **2023**, *14* (1), 7944.
(106) Peřina, J., Jr; Thapliyal, K.; Chimczak, G.; Kowalewska-Kudłaszyk, A.; Miranowicz, A. Multiple quantum exceptional, diabolical, and hybrid points in multimode bosonic systems: II. Nonconventional PT-symmetric dynamics and unidirectional coupling. *arXiv* **2024**, 2405.016667 (accessed 4-8-2024).
(107) Zhong, Q.; Kou, J.; Özdemir, S. K.; El-Ganainy, R. Hierarchical Construction of Higher-Order Exceptional Points. *Phys. Rev. Lett.* **2020**, *125* (20), 203602.
(108) Kullig, J.; Grom, D.; Klembt, S.; Wiersig, J. Higher-order exceptional points in waveguide-coupled microcavities: perturbation induced frequency splitting and mode patterns. *Photonics Research* **2023**, *11* (10), A54−A64.
(109) Ding, K.; Ma, G.; Xiao, M.; Zhang, Z. Q.; Chan, C. T. Emergence, Coalescence, and Topological Properties of Multiple Exceptional Points and Their Experimental Realization. *Physical Review X* **2016**, *6* (2), 021007.
(110) Mandal, I.; Bergholtz, E. J. Symmetry and Higher-Order Exceptional Points. *Phys. Rev. Lett.* **2021**, *127* (18), 186601.
(111) Delplace, P.; Yoshida, T.; Hatsugai, Y. Symmetry-Protected Multifold Exceptional Points and Their Topological Characterization. *Phys. Rev. Lett.* **2021**, *127* (18), 186602.
(112) Wang, K.; Xiao, L.; Lin, H.; Yi, W.; Bergholtz, E. J.; Xue, P. Experimental simulation of symmetry-protected higher-order exceptional points with single photons. *Science Advances* **2023**, *9* (34), No. eadi0732.
(113) Kim, J.; Ha, T.; Kim, D.; Lee, D.; Lee, K.-S.; Won, J.; Moon, Y.; Lee, M. Third-order exceptional point in an ion-cavity system. *Appl. Phys. Lett.* **2023**, *123* (16), 161104.
(114) Pick, A.; Zhen, B.; Miller, O. D.; Hsu, C. W.; Hernandez, F.; Rodriguez, A. W.; Soljacic, M.; Johnson, S. G. General theory of spontaneous emission near exceptional points. *Opt. Express* **2017**, *25* (11), 12325−12348.

https://doi.org/10.1021/acsnano.4c15648
ACS Nano XXXX, XXX, XXX−XXX

(115) Xiong, W.; Li, Z.; Song, Y.; Chen, J.; Zhang, G.-Q.; Wang, M. Higher-order exceptional point in a pseudo-Hermitian cavity optomechanical system. *Phys. Rev. A* **2021**, *104* (6), 063508.
(116) Xiong, W.; Li, Z.; Zhang, G.-Q.; Wang, M.; Li, H.-C.; Luo, X.-Q.; Chen, J. Higher-order exceptional point in a blue-detuned non-Hermitian cavity optomechanical system. *Phys. Rev. A* **2022**, *106* (3), 033518.
(117) Wang, C.; Jiang, X.; Zhao, G.; Zhang, M.; Hsu, C. W.; Peng, B.; Stone, A. D.; Jiang, L.; Yang, L. Electromagnetically induced transparency at a chiral exceptional point. *Nat. Phys.* **2020**, *16*, 334.
(118) Mao, W.; Fu, Z.; Li, Y.; Li, F.; Yang, L. Exceptional-point-enhanced phase sensing. *Science Advances* **2024**, *10* (14), No. eadl5037.
(119) Lu, Y.; Zhao, Y.; Li, R.; Liu, J. Anomalous spontaneous emission dynamics at chiral exceptional points. *Opt. Express* **2022**, *30* (23), 41784−41803.
(120) Berry, M. V.; Wilkinson, M. Diabolical points in the spectra of triangles. *Proceedings of the Royal Society A* **1984**, *392* (1802), 15−43.
(121) Thapliyal, K.; Peřina, J., Jr; Chimczak, G.; Kowalewska-Kudłaszyk, A.; Miranowicz, A. Multiple quantum exceptional, diabolical, and hybrid points in multimode bosonic systems: I. Inherited and genuine singularities. *arXiv* **2024**, 2405.01666 (accessed 4−8, 2024).
(122) Arkhipov, I. I.; Miranowicz, A.; Minganti, F.; Özdemir, S. K.; Nori, F. Dynamically crossing diabolic points while encircling exceptional curves: A programmable symmetric-asymmetric multi-mode switch. *Nat. Commun.* **2023**, *14* (1), 2076.
(123) Meng, H.; Ang, Y. S.; Lee, C. H. Exceptional points in non-Hermitian systems: Applications and recent developments. *Appl. Phys. Lett.* **2024**, *124* (6), 060502.
(124) Opala, A.; Furman, M.; Król, M.; Mirek, R.; Tyszka, K.; Seredyński, B.; Pacuski, W.; Szczytko, J.; Matuszewski, M.; Pietka, B. Natural exceptional points in the excitation spectrum of a light-matter system. *Optica* **2023**, *10* (8), 1111−1117.
(125) Rüter, C. E.; Makris, K. G.; El-Ganainy, R.; Christodoulides, D. N.; Segev, M.; Kip, D. Observation of parity-time symmetry in optics. *Nat. Phys.* **2010**, *6* (3), 192−195.
(126) Peng, B.; Özdemir, S. K.; Lei, F.; Monifi, F.; Gianfreda, M.; Long, G. L.; Fan, S.; Nori, F.; Bender, C. M.; Yang, L. Parity-time-symmetric whispering-gallery microcavities. *Nat. Phys.* **2014**, *10* (5), 394−398.
(127) Chang, L.; Jiang, X.; Hua, S.; Yang, C.; Wen, J.; Jiang, L.; Li, G.; Wang, G.; Xiao, M. Parity-time symmetry and variable optical isolation in active-passive-coupled microresonators. *Nat. Photonics* **2014**, *8* (7), 524−529.
(128) Doppler, J.; Mailybaev, A. A.; Bohm, J.; Kuhl, U.; Girschik, A.; Libisch, F.; Milburn, T. J.; Rabl, P.; Moiseyev, N.; Rotter, S. Dynamically encircling an exceptional point for asymmetric mode switching. *Nature* **2016**, *537* (7618), 76−79.
(129) Miller, J. L. Exceptional points make for exceptional sensors. *Phys. Today* **2017**, *70* (10), 23−26.
(130) Hodaei, H.; Miri, M. A.; Heinrich, M.; Christodoulides, D. N.; Khajavikhan, M. Parity-time-symmetric microring lasers. *Science* **2014**, *346* (6212), 975−8.
(131) Feng, L.; Wong, Z. J.; Ma, R. M.; Wang, Y.; Zhang, X. Single-mode laser by parity-time symmetry breaking. *Science* **2014**, *346* (6212), 972−5.
(132) Hodaei, H.; Miri, M.-A.; Hassan, A. U.; Hayenga, W. E.; Heinrich, M.; Christodoulides, D. N.; Khajavikhan, M. Single mode lasing in transversely multi-moded PT-symmetric microring resonators. *Laser & Photonics Reviews* **2016**, *10* (3), 494−499.
(133) Yao, R.; Lee, C.-S.; Podolskiy, V.; Guo, W. Electrically Injected Parity Time-Symmetric Single Transverse-Mode Lasers. *Laser Photonics Rev.* **2019**, *13* (1), 1800154.
(134) Hokmabadi, M. P.; Schumer, A.; Christodoulides, D. N.; Khajavikhan, M. Non-Hermitian ring laser gyroscopes with enhanced Sagnac sensitivity. *Nature* **2019**, *576* (7785), 70−74.
(135) Lai, Y.-H.; Lu, Y.-K.; Suh, M.-G.; Yuan, Z.; Vahala, K. Observation of the exceptional-point-enhanced Sagnac effect. *Nature* **2019**, *576* (7785), 65−69.
(136) Guo, A.; Salamo, G. J.; Duchesne, D.; Morandotti, R.; Volatier-Ravat, M.; Aimez, V.; Siviloglou, G. A.; Christodoulides, D. N. Observation of PT-symmetry breaking in complex optical potentials. *Phys. Rev. Lett.* **2009**, *103* (9), 093902.
(137) Peng, B.; Ozdemir, S. K.; Rotter, S.; Yilmaz, H.; Liertzer, M.; Monifi, F.; Bender, C. M.; Nori, F.; Yang, L. Loss-induced suppression and revival of lasing. *Science* **2014**, *346* (6207), 328−32.
(138) Joglekar, Y. N.; Harter, A. K. Passive parity-time-symmetry-breaking transitions without exceptional points in dissipative photonic systems [Invited]. *Photonics Research* **2018**, *6* (8), A51.
(139) Jiang, H.; Zhang, W.; Lu, G.; Ye, L.; Lin, H.; Tang, J.; Xue, Z.; Li, Z.; Xu, H.; Gong, Q. Exceptional points and enhanced nanoscale sensing with a plasmon-exciton hybrid system. *Photonics Research* **2022**, *10* (2), 557−563.
(140) Kuo, P.-C.; Lambert, N.; Miranowicz, A.; Chen, H.-B.; Chen, G.-Y.; Chen, Y.-N.; Nori, F. Collectively induced exceptional points of quantum emitters coupled to nanoparticle surface plasmons. *Phys. Rev. A* **2020**, *101* (1), 013814.
(141) Yu, S.; Meng, Y.; Tang, J.-S.; Xu, X.-Y.; Wang, Y.-T.; Yin, P.; Ke, Z.-J.; Liu, W.; Li, Z.-P.; Yang, Y.-Z.; Chen, G.; Han, Y.-J.; Li, C.-F.; Guo, G.-C. Experimental Investigation of Quantum PT-Enhanced Sensor. *Phys. Rev. Lett.* **2020**, *125* (24), 240506.
(142) Luo, X.-W.; Zhang, C.; Du, S. Quantum Squeezing and Sensing with Pseudo-Anti-Parity-Time Symmetry. *Phys. Rev. Lett.* **2022**, *128* (17), 173602.
(143) Chen, C.; Jin, L.; Liu, R.-B. Sensitivity of parameter estimation near the exceptional point of a non-Hermitian system. *New J. Phys.* **2019**, *21* (8), 083002.
(144) Mortensen, N. A.; Gonçalves, P. A. D.; Khajavikhan, M.; Christodoulides, D. N.; Tserkezis, C.; Wolff, C. Fluctuations and noise-limited sensing near the exceptional point of parity-time-symmetric resonator systems. *Optica* **2018**, *5* (10), 1342.
(145) Anderson, D.; Shah, M.; Fan, L. Clarification of the Exceptional-Point Contribution to Photonic Sensing. *Physical Review Applied* **2023**, *19* (3), 034059.
(146) Wang, Y.-Y.; Wu, C.-W.; Wu, W.; Chen, P.-X. PT-symmetric quantum sensing: Advantages and restrictions. *Phys. Rev. A* **2024**, *109* (6), 062611.
(147) Naikoo, J.; Chhajlany, R. W.; Kołodyński, J. Multiparameter Estimation Perspective on Non-Hermitian Singularity-Enhanced Sensing. *Phys. Rev. Lett.* **2023**, *131* (22), 220801.
(148) Wang, H.; Lai, Y.-H.; Yuan, Z.; Suh, M.-G.; Vahala, K. Petermann-factor sensitivity limit near an exceptional point in a Brillouin ring laser gyroscope. *Nat. Commun.* **2020**, *11* (1), 1610.
(149) Wolff, C.; Tserkezis, C.; Mortensen, N. A. On the time evolution at a fluctuating exceptional point. *Nanophotonics* **2019**, *8* (8), 1319−1326.
(150) Xu, J.; Mao, Y.; Li, Z.; Zuo, Y.; Zhang, J.; Yang, B.; Xu, W.; Liu, N.; Deng, Z. J.; Chen, W.; Xia, K.; Qiu, C.-W.; Zhu, Z.; Jing, H.; Liu, K. Single-cavity loss-enabled nanometrology. *Nat. Nanotechnol.* **2024**, *19* (10), 1472−1477.
(151) Ruan, Y.-P.; Tang, J.-S.; Li, Z.; Wu, H.; Zhou, W.; Xiao, L.; Chen, J.; Ge, S.-J.; Hu, W.; Zhang, H.; Qiu, C.-W.; Liu, W.; Jing, H.; Lu, Y.-Q.; Xia, K. Observation of loss-enhanced magneto-optical effect. *Nat. Photonics* **2025**, *19* (1), 109−115.
(152) Simonson, L.; Ozdemir, S. K.; Eisfeld, A.; Metelmann, A.; El-Ganainy, R. Nonuniversality of quantum noise in optical amplifiers operating at exceptional points. *Physical Review Research* **2022**, *4* (3), 033226.
(153) Bai, K.; Fang, L.; Liu, T.-R.; Li, J.-Z.; Wan, D.; Xiao, M. Nonlinearity-enabled higher-order exceptional singularities with ultra-enhanced signal-to-noise ratio. *National Science Review* **2023**, *10* (7), nwac259.
(154) Li, H.; Chen, L.; Wu, W.; Wang, H.; Wang, T.; Zhong, Y.; Huang, F.; Liu, G.-S.; Chen, Y.; Luo, Y.; Chen, Z. Enhanced

https://doi.org/10.1021/acsnano.4c15648
ACS Nano XXXX, XXX, XXX−XXX

sensitivity with nonlinearity-induced exceptional points degeneracy lifting. *Communications Physics* **2024**, *7* (1), 117.
(155) Peters, K. J. H.; Rodriguez, S. R. K. Exceptional Precision of a Nonlinear Optical Sensor at a Square-Root Singularity. *Phys. Rev. Lett.* **2022**, *129* (1), 013901.
(156) Li, Z.; Li, C.; Xu, G.; Chen, W.; Xiong, Z.; Jing, H.; Ho, J. S.; Qiu, C.-W. Synergetic positivity of loss and noise in nonlinear non-Hermitian resonators. *Science Advances* **2023**, *9* (27), No. eadi0562.
(157) Pelton, M. Modified spontaneous emission in nanophotonic structures. *Nat. Photonics* **2015**, *9* (7), 427−435.
(158) Ma, R.-M.; Oulton, R. F. Applications of nanolasers. *Nat. Nanotechnol.* **2019**, *14* (1), 12−22.
(159) Zhou, W.; Liu, J.; Zhu, J.; Gromyko, D.; Qiu, C.; Wu, L. Exceptional points unveiling quantum limit of fluorescence rates in non-Hermitian plexcitonic single-photon sources. *APL Quantum* **2024**, *1* (1), 016110.
(160) Purcell, E. M.; Torrey, H. C.; Pound, R. V. Resonance Absorption by Nuclear Magnetic Moments in a Solid. *Phys. Rev.* **1946**, *69* (1−2), 37−38.
(161) Wang, R.; Wang, X.-H.; Gu, B.-Y.; Yang, G.-Z. Local density of states in three-dimensional photonic crystals: Calculation and enhancement effects. *Phys. Rev. B* **2003**, *67* (15), 155114.
(162) Wang, X. H.; Kivshar, Y. S.; Gu, B. Y. Giant lamb shift in photonic crystals. *Phys. Rev. Lett.* **2004**, *93* (7), 073901.
(163) Wang, X.-H.; Gu, B.-Y.; Wang, R.; Xu, H.-Q. Decay Kinetic Properties of Atoms in Photonic Crystals with Absolute Gaps. *Phys. Rev. Lett.* **2003**, *91* (11), 113904.
(164) Garmon, S.; Ordonez, G.; Hatano, N. Anomalous-order exceptional point and non-Markovian Purcell effect at threshold in one-dimensional continuum systems. *Physical Review Research* **2021**, *3* (3), 033029.
(165) Ren, J.; Franke, S.; Hughes, S. Quasinormal Mode Theory of Chiral Power Flow from Linearly Polarized Dipole Emitters Coupled to Index-Modulated Microring Resonators Close to an Exceptional Point. *ACS Photonics* **2022**, *9* (4), 1315−1326.
(166) Ren, J.; Franke, S.; Hughes, S. Quasinormal Modes, Local Density of States, and Classical Purcell Factors for Coupled Loss-Gain Resonators. *Physical Review X* **2021**, *11* (4), 041020.
(167) Pick, A.; Lin, Z.; Jin, W.; Rodriguez, A. W. Enhanced nonlinear frequency conversion and Purcell enhancement at exceptional points. *Phys. Rev. B* **2017**, *96* (22), 224303.
(168) Zubizarreta Casalengua, E.; López Carreño, J. C.; Laussy, F. P.; Valle, E. d. Conventional and Unconventional Photon Statistics. *Laser Photonics Rev.* **2020**, *14* (6), 1900279.
(169) Imamoglu, A.; Schmidt, H.; Woods, G.; Deutsch, M. Strongly Interacting Photons in a Nonlinear Cavity. *Phys. Rev. Lett.* **1997**, *79* (8), 1467−1470.
(170) Geng, Z.; Chen, Y.; Jiang, Y.; Xia, Y.; Song, J. Engineering dynamical photon blockade with Liouville exceptional points. *Opt. Lett.* **2024**, *49* (11), 3026−3029.
(171) Choi, H.; Zhu, D.; Yoon, Y.; Englund, D. Cascaded Cavities Boost the Indistinguishability of Imperfect Quantum Emitters. *Phys. Rev. Lett.* **2019**, *122* (18), 183602.
(172) Grange, T.; Hornecker, G.; Hunger, D.; Poizat, J. P.; Gerard, J. M.; Senellart, P.; Auffeves, A. Cavity-funneled generation of indistinguishable single photons from strongly dissipative quantum emitters. *Phys. Rev. Lett.* **2015**, *114* (19), 193601.
(173) Liu, W.; Wu, Y.; Duan, C.-K.; Rong, X.; Du, J. Dynamically Encircling an Exceptional Point in a Real Quantum System. *Phys. Rev. Lett.* **2021**, *126* (17), 170506.
(174) Pick, A.; Silberstein, S.; Moiseyev, N.; Bar-Gill, N. Robust mode conversion in NV centers using exceptional points. *Physical Review Research* **2019**, *1* (1), 013015.
(175) Tang, Z.; Chen, T.; Zhang, X. Highly Efficient Transfer of Quantum State and Robust Generation of Entanglement State Around Exceptional Lines. *Laser Photonics Rev.* **2024**, *18* (4), 2300794.
(176) Abbasi, M.; Chen, W.; Naghiloo, M.; Joglekar, Y. N.; Murch, K. W. Topological Quantum State Control through Exceptional-Point Proximity. *Phys. Rev. Lett.* **2022**, *128* (16), 160401.
(177) Purkayastha, A.; Kulkarni, M.; Joglekar, Y. N. Emergent PT symmetry in a double-quantum-dot circuit QED setup. *Physical Review Research* **2020**, *2* (4), 043075.
(178) Liao, Q.; Leblanc, C.; Ren, J.; Li, F.; Li, Y.; Solnyshkov, D.; Malpuech, G.; Yao, J.; Fu, H. Experimental Measurement of the Divergent Quantum Metric of an Exceptional Point. *Phys. Rev. Lett.* **2021**, *127* (10), 107402.
(179) Graefe, E.-M. PT symmetry dips into two-photon interference. *Nat. Photonics* **2019**, *13* (12), 822−823.
(180) Yuan, H. Y.; Yan, P.; Zheng, S.; He, Q. Y.; Xia, K.; Yung, M.-H. Steady Bell State Generation via Magnon-Photon Coupling. *Phys. Rev. Lett.* **2020**, *124* (5), 053602.
(181) Zhang, J.; Zhou, Y.-L.; Zuo, Y.; Zhang, H.; Chen, P.-X.; Jing, H.; Kuang, L.-M. Exceptional Entanglement and Quantum Sensing with a Parity-Time-Symmetric Two-Qubit System. *Advanced Quantum Technologies* **2024**, *7* (5), 2300350.
(182) Li, C.; Song, Z. Generation of Bell, W, and Greenberger-Horne-Zeilinger states via exceptional points in non-Hermitian quantum spin systems. *Phys. Rev. A* **2015**, *91* (6), 062104.
(183) Masharin, M. A.; Oskolkova, T.; Isik, F.; Volkan Demir, H.; Samusev, A. K.; Makarov, S. V. Giant Ultrafast All-Optical Modulation Based on Exceptional Points in Exciton-Polariton Perovskite Metasurfaces. *ACS Nano* **2024**, *18* (4), 3447−3455.
(184) Lau, H. K.; Clerk, A. A. Fundamental limits and non-reciprocal approaches in non-Hermitian quantum sensing. *Nat. Commun.* **2018**, *9* (1), 4320.
(185) Peterson, J. P. S.; Batalhão, T. B.; Herrera, M.; Souza, A. M.; Sarthour, R. S.; Oliveira, I. S.; Serra, R. M. Experimental Characterization of a Spin Quantum Heat Engine. *Phys. Rev. Lett.* **2019**, *123* (24), 240601.
(186) Zhang, J. W.; Zhang, J. Q.; Ding, G. Y.; Li, J. C.; Bu, J. T.; Wang, B.; Yan, L. L.; Su, S. L.; Chen, L.; Nori, F.; Özdemir, S. K.; Zhou, F.; Jing, H.; Feng, M. Dynamical control of quantum heat engines using exceptional points. *Nat. Commun.* **2022**, *13* (1), 6225.
(187) Bu, J.-T.; Zhang, J.-Q.; Ding, G.-Y.; Li, J.-C.; Zhang, J.-W.; Wang, B.; Ding, W.-Q.; Yuan, W.-F.; Chen, L.; Zhong, Q.; Keçebas, A.; Özdemir, S. K.; Zhou, F.; Jing, H.; Feng, M. Chiral quantum heating and cooling with an optically controlled ion. *Light: Science & Applications* **2024**, *13* (1), 143.
(188) Insinga, A.; Andresen, B.; Salamon, P.; Kosloff, R. Quantum heat engines: Limit cycles and exceptional points. *Phys. Rev. E* **2018**, *97* (6), 062153.
(189) Choi, Y.; Hahn, C.; Yoon, J. W.; Song, S. H.; Berini, P. Extremely broadband, on-chip optical nonreciprocity enabled by mimicking nonlinear anti-adiabatic quantum jumps near exceptional points. *Nat. Commun.* **2017**, *8* (1), 14154.
(190) Downing, C. A.; Carreno, J. C. L.; Laussy, F. P.; del Valle, E.; Fernandez-Dominguez, A. I. Quasichiral Interactions between Quantum Emitters at the Nanoscale. *Phys. Rev. Lett.* **2019**, *122* (5), 057401.
(191) Söllner, I.; Mahmoodian, S.; Hansen, S. L.; Midolo, L.; Javadi, A.; Kiršanskė, G.; Pregnolato, T.; El-Ella, H.; Lee, E. H.; Song, J. D.; Stobbe, S.; Lodahl, P. Deterministic photon-emitter coupling in chiral photonic circuits. *Nat. Nanotechnol.* **2015**, *10* (9), 775−778.
(192) Ren, Y.-L.; Ma, S.-L.; Xie, J.-K.; Li, F.-L. Nonreciprocal photonic quantum router via synthetic magnetism. *Appl. Phys. Lett.* **2023**, *122* (24), 244002.
(193) Shlesinger, I.; Vandersmissen, J.; Oksenberg, E.; Verhagen, E.; Koenderink, A. F. Hybrid cavity-antenna architecture for strong and tunable sideband-selective molecular Raman scattering enhancement. *Science Advances* **2023**, *9* (51), No. eadj4637.
(194) Guria, C.; Zhong, Q.; Ozdemir, S. K.; Patil, Y. S. S.; El-Ganainy, R.; Harris, J. G. E. Resolving the topology of encircling multiple exceptional points. *Nat. Commun.* **2024**, *15* (1), 1369.

https://doi.org/10.1021/acsnano.4c15648
ACS Nano XXXX, XXX, XXX−XXX

(195) Midya, B.; Zhao, H.; Feng, L. Non-Hermitian photonics promises exceptional topology of light. *Nat. Commun.* **2018**, *9* (1), 2674.
(196) Hou, C.; Li, L.; Wu, G.; Ruan, Y.; Chen, S.; Baronio, F. Topological edge states in one-dimensional non-Hermitian Su-Schrieffer-Heeger systems of finite lattice size: Analytical solutions and exceptional points. *Phys. Rev. B* **2023**, *108* (8), 085425.
(197) Li, J.; Gong, Z. Alternating quantum-emitter chains: Exceptional-point phase transition, edge state, and quantum walks. *Phys. Rev. A* **2024**, *109* (2), 023718.
(198) Nakagawa, M.; Kawakami, N.; Ueda, M. Exact Liouvillian Spectrum of a One-Dimensional Dissipative Hubbard Model. *Phys. Rev. Lett.* **2021**, *126* (11), 110404.
(199) Zhang, X.; Gong, J. Non-Hermitian Floquet topological phases: Exceptional points, coalescent edge modes, and the skin effect. *Phys. Rev. B* **2020**, *101* (4), 045415.
(200) He, P.; Huang, Z.-H. Floquet engineering and simulating exceptional rings with a quantum spin system. *Phys. Rev. A* **2020**, *102* (6), 062201.
(201) Kiselev, E. I.; Rudner, M. S.; Lindner, N. H. Inducing exceptional points, enhancing plasmon quality and creating correlated plasmon states with modulated Floquet parametric driving. *Nat. Commun.* **2024**, *15* (1), 9914.
(202) Nair, J. M. P.; Mukhopadhyay, D.; Agarwal, G. S. Enhanced Sensing of Weak Anharmonicities through Coherences in Dissipatively Coupled Anti-PT Symmetric Systems. *Phys. Rev. Lett.* **2021**, *126* (18), 180401.
(203) Zhao, J.; Liu, Y.; Wu, L.; Duan, C.-K.; Liu, Y.-x.; Du, J. Observation of Anti-PT-Symmetry Phase Transition in the Magnon-Cavity-Magnon Coupled System. *Physical Review Applied* **2020**, *13* (1), 014053.
(204) Zhang, F.; Feng, Y.; Chen, X.; Ge, L.; Wan, W. Synthetic Anti-PT Symmetry in a Single Microcavity. *Phys. Rev. Lett.* **2020**, *124* (5), 053901.
(205) Xu, X.-W.; Liao, J.-Q.; Jing, H.; Kuang, L.-M. Anti-parity-time symmetry hidden in a damping linear resonator. *Science China Physics, Mechanics & Astronomy* **2023**, *66* (10), 100312.
(206) Zhang, S. M.; Zhang, X. Z.; Jin, L.; Song, Z. High-order exceptional points in supersymmetric arrays. *Phys. Rev. A* **2020**, *101* (3), 033820.
(207) Budich, J. C.; Bergholtz, E. J. Non-Hermitian Topological Sensors. *Phys. Rev. Lett.* **2020**, *125* (18), 180403.
(208) Koch, F.; Budich, J. C. Quantum non-Hermitian topological sensors. *Physical Review Research* **2022**, *4* (1), 013113.
(209) Wu, X.; Wang, Z.; Yang, F.; Gao, R.; Liang, C.; Tey, M. K.; Li, X.; Pohl, T.; You, L. Dissipative time crystal in a strongly interacting Rydberg gas. *Nat. Phys.* **2024**, *20* (9), 1389−1394.
(210) Li, Y.; Wang, C.; Tang, Y.; Liu, Y.-C. Time Crystal in a Single-Mode Nonlinear Cavity. *Phys. Rev. Lett.* **2024**, *132* (18), 183803.
(211) Chen, Y.-H.; Zhang, X. Realization of an inherent time crystal in a dissipative many-body system. *Nat. Commun.* **2023**, *14* (1), 6161.
(212) Guidry, M. A.; Lukin, D. M.; Yang, K. Y.; Trivedi, R.; Vučković, J. Quantum optics of soliton microcombs. *Nat. Photonics* **2022**, *16* (1), 52−58.
(213) Bin, Q.; Qiu, Q.-Y.; Wu, Y.; Lü, X.-Y. Entangled Photon-Magnon Bundle Emission. *Laser Photonics Rev.* **2024**, *18* (9), 2300977.
(214) Muñoz, C. S.; del Valle, E.; Tudela, A. G.; Müller, K.; Lichtmannecker, S.; Kaniber, M.; Tejedor, C.; Finley, J. J.; Laussy, F. P. Emitters of N-photon bundles. *Nat. Photonics* **2014**, *8* (7), 550−555.
(215) Roy, A.; Jahani, S.; Guo, Q.; Dutt, A.; Fan, S.; Miri, M.-A.; Marandi, A. Nondissipative non-Hermitian dynamics and exceptional points in coupled optical parametric oscillators. *Optica* **2021**, *8* (3), 415−421.
(216) Laha, A.; Dey, S.; Gandhi, H. K.; Biswas, A.; Ghosh, S. Exceptional Point and toward Mode-Selective Optical Isolation. *ACS Photonics* **2020**, *7* (4), 967−974.
(217) Song, P.; Ruan, X.; Ding, H.; Li, S.; Chen, M.; Huang, R.; Kuang, L.-M.; Zhao, Q.; Tsai, J.-S.; Jing, H.; Yang, L.; Nori, F.; Zheng, D.; Liu, Y.-x.; Zhang, J.; Peng, Z. Experimental realization of on-chip few-photon control around exceptional points. *Nat. Commun.* **2024**, *15* (1), 9848.
(218) Choi, H.; Heuck, M.; Englund, D. Self-Similar Nanocavity Design with Ultrasmall Mode Volume for Single-Photon Nonlinearities. *Phys. Rev. Lett.* **2017**, *118* (22), 223605.
(219) Barreda, A.; Mercadé, L.; Zapata-Herrera, M.; Aizpurua, J.; Martínez, A. Hybrid Photonic-Plasmonic Cavity Design for Very Large Purcell Factors at Telecommunication Wavelengths. *Physical Review Applied* **2022**, *18* (4), 044066.
(220) Vaianella, F.; Hamm, J. M.; Hess, O.; Maes, B. Strong Coupling and Exceptional Points in Optically Pumped Active Hyperbolic Metamaterials. *ACS Photonics* **2018**, *5* (6), 2486−2495.
(221) Sang, Y.; Wang, C.-Y.; Raja, S. S.; Cheng, C.-W.; Huang, C.-T.; Chen, C.-A.; Zhang, X.-Q.; Ahn, H.; Shih, C.-K.; Lee, Y.-H.; Shi, J.; Gwo, S. Tuning of Two-Dimensional Plasmon-Exciton Coupling in Full Parameter Space: A Polaritonic Non-Hermitian System. *Nano Lett.* **2021**, *21* (6), 2596−2602.
(222) Xomalis, A.; Zheng, X.; Chikkaraddy, R.; Koczor-Benda, Z.; Miele, E.; Rosta, E.; Vandenbosch, G. A. E.; Martínez, A.; Baumberg, J. J. Detecting mid-infrared light by molecular frequency upconversion in dual-wavelength nanoantennas. *Science* **2021**, *374* (6572), 1268−1271.
(223) Scully, M. O.; Chapin, K. R.; Dorfman, K. E.; Kim, M. B.; Svidzinsky, A. Quantum heat engine power can be increased by noise-induced coherence. *Proc. Natl. Acad. Sci. U. S. A.* **2011**, *108* (37), 15097−15100.
(224) Benz, F.; Schmidt, M. K.; Dreismann, A.; Chikkaraddy, R.; Zhang, Y.; Demetriadou, A.; Carnegie, C.; Ohadi, H.; de Nijs, B.; Esteban, R.; Aizpurua, J.; Baumberg, J. J. Single-molecule optomechanics in 'picocavities'. *Science* **2016**, *354* (6313), 726−729.

https://doi.org/10.1021/acsnano.4c15648
ACS Nano XXXX, XXX, XXX−XXX